

Copyright
by
Xinggang Christopher Liu
2015

**The Thesis Committee for Xinggang Christopher Liu
Certifies that this is the approved version of the following thesis:**

**Stratigraphy, Depositional History, and Pore Network of the Lower
Cretaceous Sunniland Carbonates in the South Florida Basin**

**APPROVED BY
SUPERVISING COMMITTEE:**

Supervisor:

Charles Kerans

Co-Supervisor:

Robert Loucks

William Fisher

**Stratigraphy, Depositional History, and Pore Network of the Lower
Cretaceous Sunniland Carbonates in the South Florida Basin**

by

Xinggang Christopher Liu, B.S., M.S.

Thesis

Presented to the Faculty of the Graduate School of

The University of Texas at Austin

in Partial Fulfillment

of the Requirements

for the Degree of

Master of Science in Energy and Earth Resources

The University of Texas at Austin

December 2015

Dedication

To mom and dad, who are the best parents ever and whom I love most dearly.

To Bill and Charlie, who inspired my passion for geology and law.

Acknowledgements

Thanks to my life mentor, William Fisher. He is like a holy gardener who makes our soul blossom.

Thanks to my advisor, Charlie Kerans for his great patience in guiding me through this project. It was the experience and opportunity from him shaped my character, pushed me through this. If it wasn't for him, none of this would be possible. I think, in the league of geology, he is the best coach ever because his righteousness and dedication to teaching and research are surpassed by none.

Thanks to my advisor, Bob Loucks for his teaching and the opportunity of this exciting project. Without his support, this thesis just would not happen.

Thanks to Wonsuck Kim and Hillary Olson for the opportunities to work as their teaching assistant. Thanks to every student in our class for their excellence and hard work. They always make my job easier than I expect.

Thanks to Michael Mosser and Natalia Blinkova for their great mentorship and teaching. They inspired my interest in philosophy of law.

Thanks to Jessica Smith, Maurine Riess, Adam Papendiek, and Stephaine Lane for their encouragement and continual support.

Thanks to my friends, Gregory Hurd, Reynaldy Fifariz, Ahmed Hassan, Benjamin Smith, and Nathan Tinker for the kind help, particularly when I struggled the most.

Thanks to every student in the Jackson School who took sequence stratigraphy and carbonate depositional environment in 2014. The love of geology made us to push each other hard to grow together. I love you all and I thank you all.

Abstract

Stratigraphy, Depositional History, and Pore Network of the Lower Cretaceous Sunniland Carbonates in the South Florida Basin

The University of Texas at Austin, 2015

Supervisors: Charles Kerans and Robert Loucks

The South Florida Basin of the eastern Gulf of Mexico represents a vast, undisturbed carbonate system that extended from the Florida Keys through the Tampa-Sarasota Arch. In South Florida, extensive subsurface data and analogous modern environments provide an opportunity to unravel the evolution of this system from shoreline to shelf-margin. This study examines the changing facies and the pore network of the Latest Aptian-Early Albian Sunniland interval. Stratigraphic results are closely comparable with contemporary carbonate platform studies in the northern Gulf of Mexico.

The Sunniland Formation was deposited during a major transgressive-regressive sequence. The Sunniland interval is divided into five third-fourth order, transgressive-regressive depositional cycles (S-1 to S-5) in south Florida using sequence analysis of shelf-interior facies succession. In these sequences, facies proportion, faunal composition, and stratal geometries of the shelf-interior are found to be the result of the changing accommodation trends and ocean chemistry. As in the Comanche Platform in South Texas, the detrimental effects of oceanic anoxic event 1B may fundamentally drive the evolution of platform morphology in the eastern Gulf of Mexico as:

- Rimmed shelf (crisis phase: S1)
- Distally steepened ramp (anoxic/dysoxic phase: S2, recovery phase: S3, S4)
- High-angle rimmed shelf (recovery to equilibrium phase: S5).

Within this hydrocarbon-producing trend, the lowered sea level at the end of S4 enhances the reservoir quality in the high-energy settings including back-reef debris aprons, tidal shoal-complex and carbonate beach by dissolution. The tight sabkha-tidal flat facies in S5 forms the reservoir seal, whereas the medium-fine crystalline dolomites in S3 may not adversely affect and likely facilitate the migration of hydrocarbon self-sourced from the high TOC, argillaceous mudstone in S2.

Table of Contents

List of Tables	xi
List of Figures	xii
Introduction.....	1
Geological Setting.....	2
The Florida Shelf	2
The Sunniland Formation	2
The Sunniland Trend.....	3
Previous Work	8
Methods and Data	18
Lithofacies.....	20
Introduction.....	20
Sabkha-hypersaline lagoon	21
Facies A: Nodular, mosaic anhydrite with dolomite lenses.....	21
Peritidal mudstone to grainstone.....	23
Facies Ct. P: Intraclastic Lime Packstone/Rudstone.....	23
Facies Rt. P: Rooted lime packstone.....	23
Facies M/W: Mollusk mudstone/wackestone	23
Mudstone/Wackestone	26
Facies Arg. M: Argillaceous mudstone	26
Cyclic Subtidal Shelf Wackestone-Packstone	28

Facies Orb. W/P: Orbitolina-skeletal wackestone/packstone	28
Facies Mil. W/P: Miliolid-skeletal wackestone/packstone	30
Shelf-interior bioherm/biostrome.....	32
Facies R. B: Rudist bafflestone.....	32
Facies R. F: Rudist floatstone	34
Facies R. R: Rudist rudstone.....	34
Facies Mon. Chon. F: Monopleurid/chondrodont floatstone.....	34
Molluscan Grainstone Shoreface/Shoal	39
Facies Orb. G: <i>Orbitolina</i> -skeletal grainstone	39
Facies Mil. G: Peloid-miliolid-grainstone	39
Facies Ooi. G: Ooid-mollusk grainstone	40
Depositional Model.....	43
Ocean Anoxic Event 1B.....	46
Stratigraphy.....	48
Summary of Approach.....	48
General Statement.....	49
Sunniland Depositional Cycle-1 (crisis phase).....	54
Sunniland Depositional Cycle-2 (anoxic/dysoxic phase)	55
Sunniland Depositional Cycle-3 (recovery phase)	55
Sunniland Depositional Cycle-4 (recovery phase)	56
Sunniland Depositional Cycle-5 (recovery to equilibrium phase).....	57

Pore Network	59
Conclusion	61
Appendix A.....	62
References.....	74

List of Tables

Table 1: Facies associations and names.....	20
---	----

List of Figures

Figure 1: Map showing Florida Peninsula Province (USGS Province 50).....	4
Figure 2: Generalized stratigraphic column.....	5
Figure 3: Location of study area	6
Figure 4: Location map of previous studies.....	7
Figure 5: Depositional environments across the Stuart City Trend, South Texas..	9
Figure 6: A. Model of the two major trends in the Sunniland Formation.	11
Figure 7: Map of Richards (1988)'s Study Area	12
Figure 8: Cross-Section A-A' by Richards (1988).	13
Figure 9: Mural Limestone ramp interior depositional model.....	17
Figure 10: Anhydrites with dolomite lenses.	22
Figure 11: Intraclastic lime rudstone.	24
Figure 12: Rooted lime packstone	25
Figure 13: Argillaceous mudstone.	27
Figure 14: Orbitolina-skeletal wackestone/packstone..	29
Figure 15: Miliolid-skeletal wackestone/packstone.....	31
Figure 16: Rudist baffestone.....	33
Figure 17: Rudist floatstone.....	36
Figure 18: Rudist rudstone.....	37
Figure 19: Monopleurid/Chondrodont floatstone.	38
Figure 20: Orbitolina-skeletal grainstone.	41
Figure 21: Miliolid-peloid grainstone.....	41
Figure 22: Ooid-mollusk grainstone	42
Figure 23: Sunniland ramp interior depositional environments.	45
Figure 24: Phelps' Schematic four-stage model	47
Figure 25: Sunniland sequence stratigraphic model	50
Figure 26: Sunniland lithofacies maps S-2 to S-5	51
Figure 27: Sunniland cross section along the blue line.....	52

Figure 28: Sunniland cross section along the red line	53
Figure 29: Dolomitized Rudist Bafflestone	60
Figure 30: Dolomitized Skeletal Wackestone.....	60

Introduction

The Sunniland Formation in the South Florida Basin holds the only hydrocarbon-producing reservoirs in South Florida (Figure 1). The current understanding of the Sunniland carbonates is at a resolution that is too low to detect subtle significant differences in facies and rock quality. Thus, further core studies are necessary to define complex facies relationships, stacking patterns and to tie those facies successions directly to petrophysical logs, thereby allowing for the identification of the lateral discontinuous environments and high-resolution reservoir architectures.

The purpose of this study is to describe Sunniland carbonates, to interpret the depositional setting of these rocks, to place the reservoir succession of this study in a larger geological context with other Sunniland reservoirs across the South Florida Basin, and to enable a better understanding on how the Florida shelf evolved in the basin. These interpretations depend on detailed studies of core data, and thin-section analysis, and integration with well logs from Felda fields (Figure 1 C; Figure 3).

The development of all Sunniland producing fields in South Florida was initiated by shelf failure or drowning on the northeastern border of the South Florida Basin (Richards, 1988). However, the study on the temporal and spatial variability of the barrier reefs along the Florida Escarpment during Cretaceous time is currently limited. This is crucial for the success of potential federal-offshore-lands bidders in the Eastern Planning Area. The more detailed study on the temporal and spatial variability of the Comanche Platform in Texas can bring some insights on the driving mechanisms and long-term response of the Florida shelf relative to the overall framework of Gulf of Mexico during Cretaceous time, potentially informing for new exploration strategies in Eastern Gulf of Mexico.

Geological Setting

THE FLORIDA SHELF

Following the breakup of Pangea and the opening of the Gulf of Mexico, the basement geometry of the Eastern Gulf of Mexico developed in Late Triassic time (Gregg, 2014). The most prominent positive basement structure, the Peninsular Arch (Figure 1), is a crystalline basement high plunging south-southeast along the axis of the Florida Peninsula (Pollastro and Viger, 1998). Since the Jurassic, the continuous deposition onlapping the Peninsular Arch formed the Florida Shelf that is separated from the deep Gulf Basin by the Florida Escarpment. Basement-involved paleotopographic highs such as the Middle Ground Arch, Tampa-Sarasota Arch, and Pine Key Arch further subdivided the Florida Shelf into the Apalachicola Embayment, Tampa Embayment, and South Florida Basin. Among other Gulf of Mexico Basins, the South Florida Basin (Figure 1, A) is unique for its continuous carbonate-evaporite deposition in a moderately restricted, shelf-interior environment. It incorporates one-third or more of the peninsula of Florida including the Florida Keys and the easternmost Gulf of Mexico. As described by Pollastro (1995), the major surrounding positive structural elements are the Tampa-Sarasota Arch, Charlotte High, 40 Mile Bend High, Largo High, and the Pine Key Arch.

THE SUNNILAND FORMATION

The Sunniland Formation (Figure 2) is dominantly a marine carbonate succession deposited in the South Florida Basin during the Lower Cretaceous. It represents the basal unit of the Ocean Reef Group of upper Trinity age, part of the Comanchean Series (Richards, 1988). The Sunniland overlies the Punta Gorda anhydrite and underlies anhydrites of the Lake Trafford Formation (Feitz, 1976). The Sunniland Formation is equivalent to the Glen Rose Formation in Texas and Mural Limestone in Arizona (Aisner, 2010). In a sequence stratigraphic framework, it is part of the upper Bexar supersequence and lower Glen Rose supersequence, roughly 112-104 Ma (Phelps, 2011).

THE SUNNILAND TREND

During the Early Cretaceous, the onshore portion of the South Florida Basin has a relatively uniform thickness with no major faults. Yet, some subtle effects from the Triassic/Jurassic igneous basement may exist as subtle topographic highs throughout the Cretaceous (Oglesby, A Gravity Profile of the South Florida Shelf, 1967). The shallower, high-energy deposition associated with these topographic highs afforded good conditions to develop the northwest-southeast Sunniland Trend (Figure 1, B) of bioherms, biostromes (patch reefs), and grain shoals. This trend is parallel with the north-northeastern boundary of the South Florida basin. Regionally, facies within the Sunniland Trend range from open-marine to shallow-water carbonates. The Sunniland Fm. starts with the sharp contact between Punta Gorda Anhydrite and an immediately overlying intraclast rudstone retrograding to the dark carbonate. After the maximum flooding interval of subtidal shelf wackestone-packstone and within *Orbitolina*-peloid packstone/grainstone, the trend of bioherms, biostromes (patch reefs), and grain shoals started to develop during the early highstand of the Sunniland transgressive-regressive sequence. Once the most significant subaerial exposure of the fragmented rudist mounds occurred, a series of intercalated sabkha-supratidal and intertidal sediments marked the transitional contact with the overlying Lake Trafford Formation.

The updip boundary of the Sunniland Trend is defined by the dominance of micritic limestone with absence of reservoir mounds, lagoonal-mudflat facies in the upper Sunniland Formation. The downdip boundary of the Sunniland Trend is marked by the complete replacement of the Sunniland limestone interval by an anhydrite-cemented, nonporous, sabkha-like facies (Oglesby, 1965). The Felda Sunniland Unit (FSU) in this study (Figure 3, also see area C, Figure 1) is located in the northern section of the Sunniland Trend. The study area is located in Lee, Hendry, and Collier Counties, southwest Florida, in the northern part of the South Florida Basin. It covers the entire Sunoco Felda, mid-Felda, and West Felda fields.



Figure 1: Map showing Florida Peninsula Province (USGS Province 50) with major positive structural elements of the South Florida Basin. A: South Florida Basin. B: Sunniland Trend. C: Felda Sunniland Unit. Modified after Pollastro (1995), Pollastro and Viger (1998), and Pollastro et al. (2000).

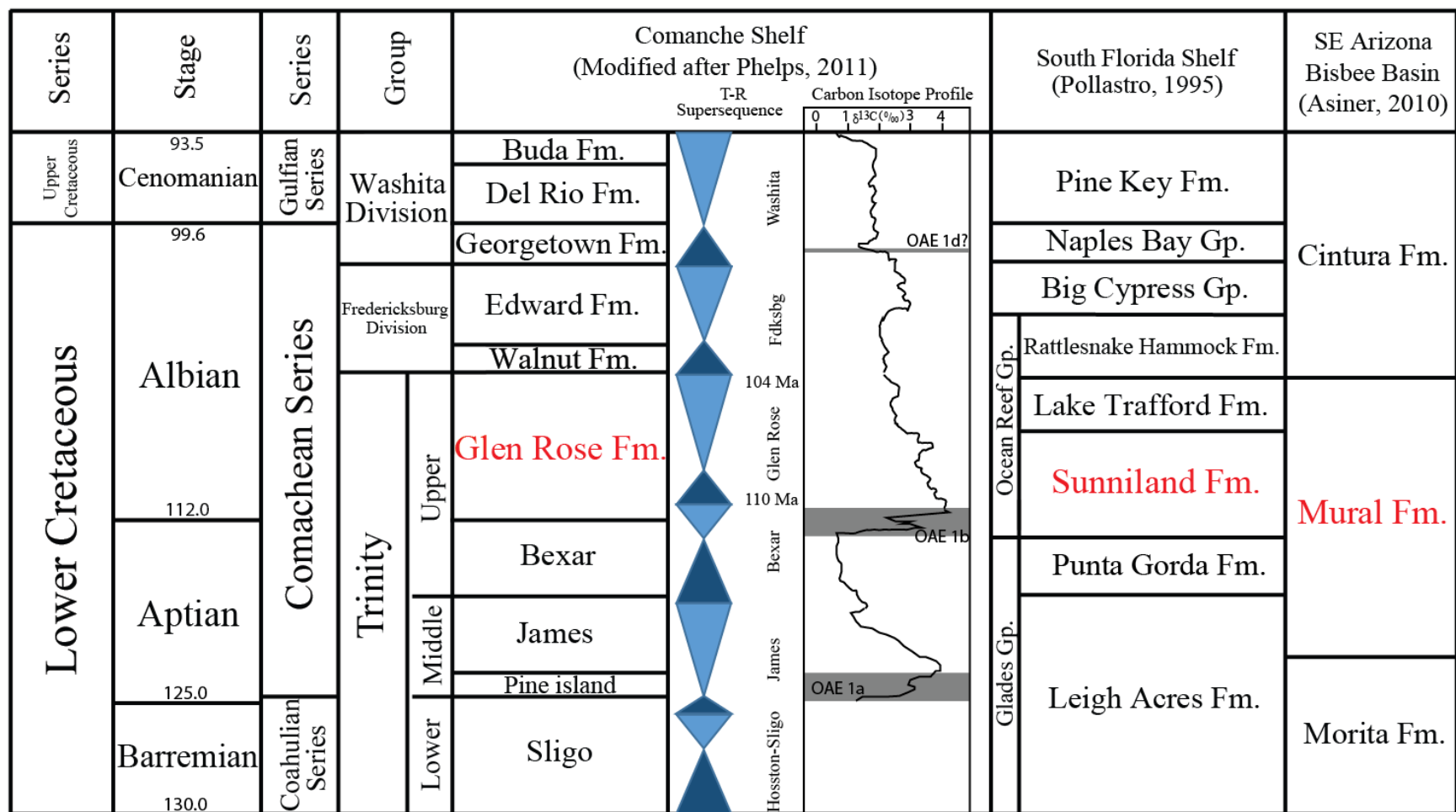


Figure 2: Generalized stratigraphic column with the position of the Sunniland Formation relative to regional and international chronostratigraphic charts.

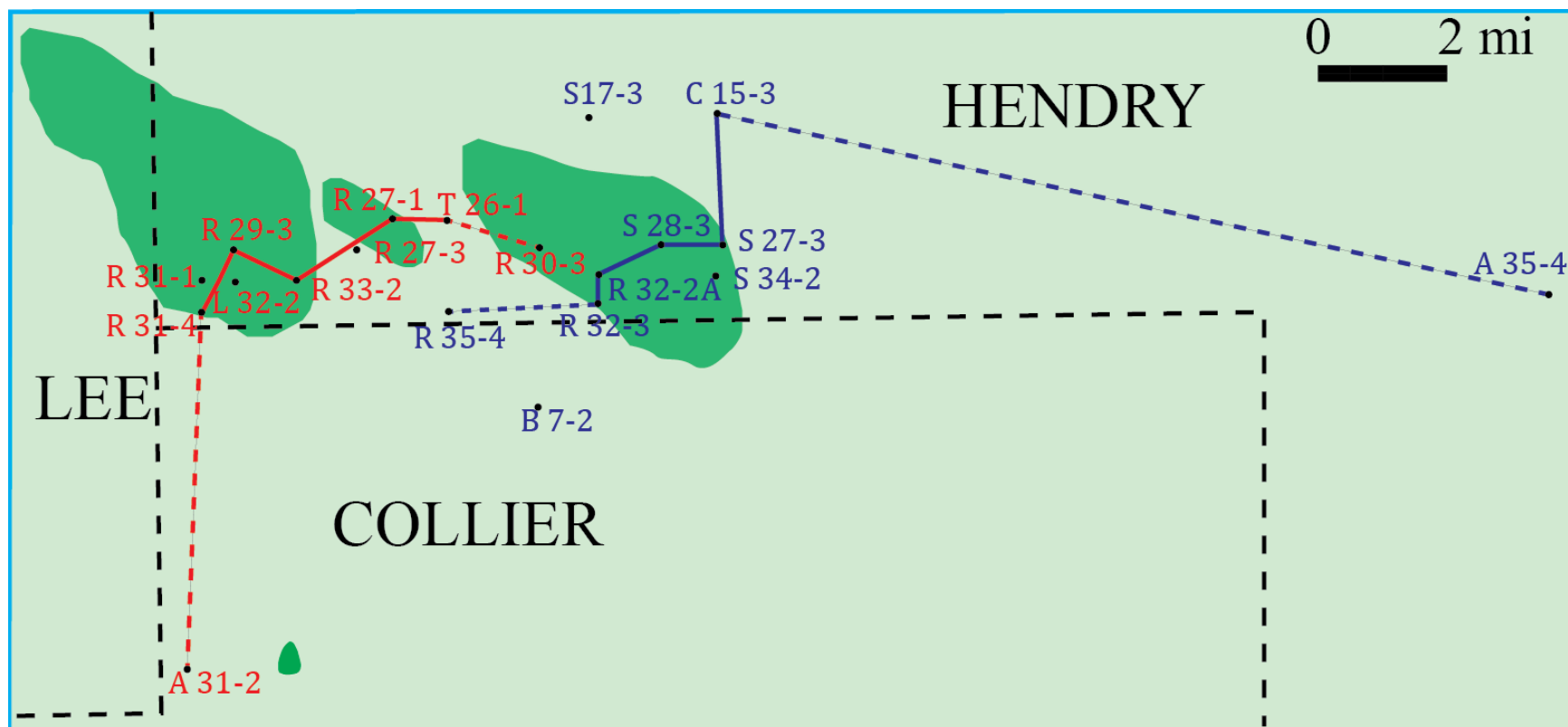


Figure 3: Location of study area showing well data in the Lee, Collier, and Hendry Counties.



Figure 4: Location map of previous studies conducted in South Florida, South Texas, and Southwest Arizona that have described the Albian rudist buildups.

Previous Work

Following the first Sunniland Formation oil field discovery in 1943, researchers associated with the Florida Geological Survey and oil companies began extensive research into the occurrence of oil and structural features of the Florida Shelf. While some authors elaborated on prospecting methods such as exploration gravity profile (Oglesby, A Gravity Profile of the South Florida Shelf, 1967) and geothermal gradients (Griffin, 1969), others linked laterally equivalent formations or mapped post-Triassic/Jurassic lithofacies relationships (Pressler, 1947; Puri and Banks, 1959; Appline and Appline, 1965; Rainwater, 1971). Winston (1971) first generated a Sunniland lithological cycle correlated with frequently repeated wireline logs responses, spurring future workers to interpret field specific Sunniland Formation data with respect to the dominant physical or biological processes within the Sunniland northwest-southeast trending band (Means, 1976; Tyler, 1976; Feitz, 1976; Applegate, 1978).

In south Texas, the Stuart City Trend was a shallow-water carbonate complex of reefs, banks, bars and island developed on a broad shelf, which encircled the Gulf of Mexico of the Lower Cretaceous. Bebout and Loucks (1974) described the depositional facies and environments present along the Stuart City Trend, Lower Cretaceous of South Texas and developed a depositional model for hydrocarbon exploration along the trend (Figure 5). In this model, the upper shelf slope is dominated by caprinid-coral wackestone with open-marine fauna. Behind the caprinid-coral patch reefs and banks, the common migratory features are beach, tidal bars, splits, channel fill and stable grain flat with water depth less than 10 feet on the shelf margin. The shallow-water shelf lagoon commonly consists of miliolid wackestone, mollusk wackestone, toucasids wackestone, and mollusk-miliolids grainstone. This model has been used in many studies of Lower Cretaceous shallow-water carbonate rocks and was very useful for understanding initial observations during data collection in this study.

Much of the subsurface and petrographic work on the Suniland Fm. has been completed on fields located within the Sunniland Trend by Mitchell-Tapping (1984; 1985; 1986; 1987, 2002, 2003), Loucks (1985), Ferber (1985), and Richards (1988).

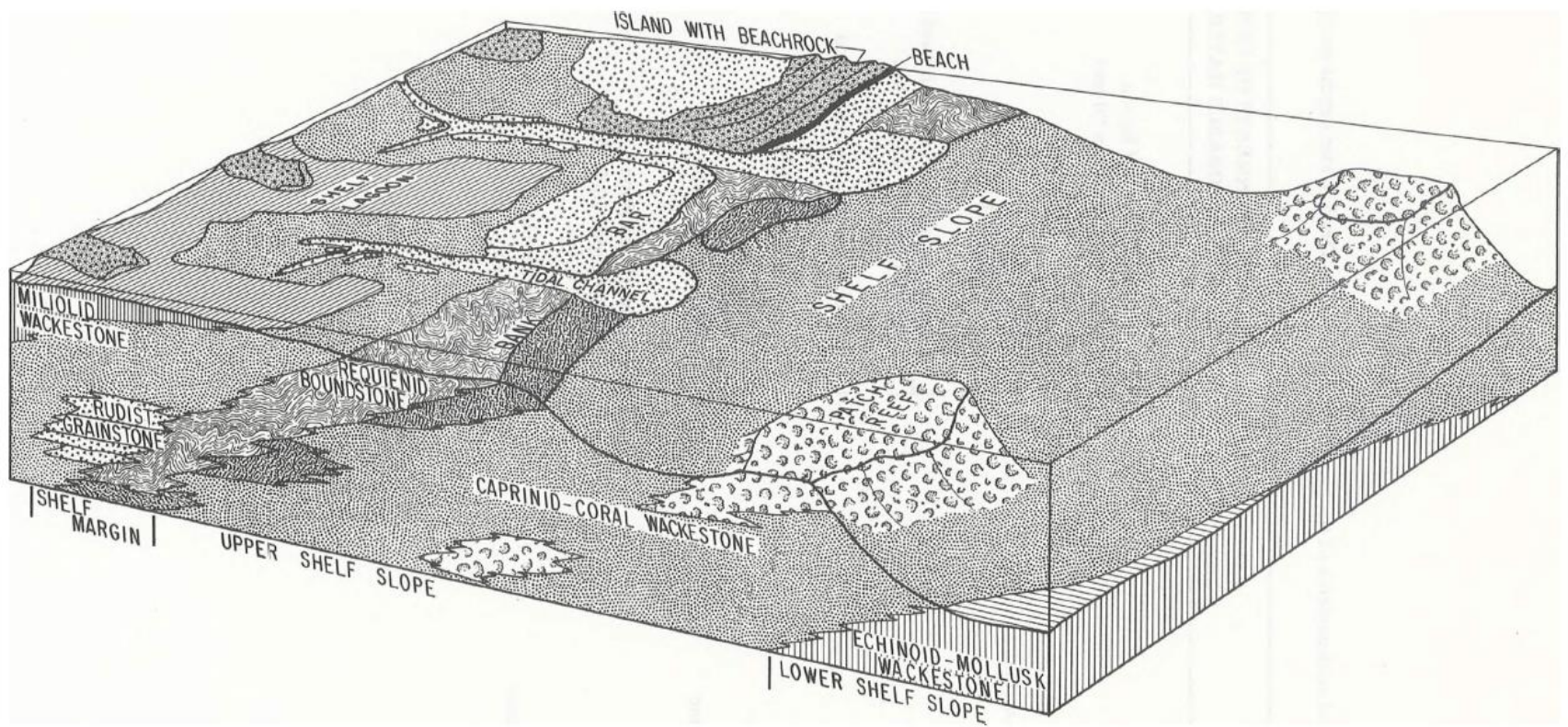


Figure 5: Facies and interpreted depositional environments across the Stuart City Trend, South Texas (Bebout and Loucks, 1974)

These examinations of the Sunniland Formation improved the understanding of the depositional history and also recognized different diagenetic phases. The study published by Loucks (1985) is so far the only published petrology study on the vertical facies sequences of the Sunniland reef core and the gradual transgression over the underlying Punta Gorda Formation at the high frequency cycle scale. The Natural Resource Management Corporation No. 31-2 Alico well (A31-2,) (see Figure 3) in Loucks' study penetrates through the caprinid bafflestone complex and the top section of the Punta Gorda anhydrite. Loucks also pointed out that the anhydrite section is similar to the age-equivalent Ferry Lake anhydrite described by Loucks and Longman (1982) in the study of Fairway field, Lower Cretaceous of East Texas. The Alico A31-2 is also included in this study and located approximately five miles south of the Sunoco-Felda Field. With close reference to previous work in Texas, Ferber (1985) interpreted that the Sunniland Formation at the Lehigh Park Field (Figure 4) was deposited during a transgressive-regressive sequence in five major depositional systems: shallow-water shelf, shoal-water carbonate complex, restricted and open lagoon, tidal flat, and sabkha and were diagenetically overprinted by dolomite and anhydrite.

Mitchell-Tapping (1984; 1985) investigated the petrology of the Sunniland Field, Forty Mile Bend Field, and the Bear Island Field and interpreted the reservoir rocks of these three fields (Figure 4) to be a barrier tidal-shoal bar, deposited near a landward mudflat area and well behind the main reef crest at the edge of the Florida escarpment. With reference to Mean's (1977) work on the Sunoco Felda Field and the West Felda Field, Mitchell-Tapping (1986) analyzed these two fields based on petrological and petrophysical information obtained from the cores and logs and developed a diagrammatic cross-section of the Sunoco Felda field. In 1987, Mitchell-Tapping pointed out that the Sunniland depositional environments are similar to those of present-day Florida Bay or the leeward side of Abaco Island and proposed the application of the tidal mudflat model to interpret part of the Sunniland depositional environment as the shallow-water, tidal mudflat in an updip part of the Bahamas Basin. More than a decade later, Mitchell-Tapping and Mitchell-Tapping (2003) re-examined the Sunoco Felda Field and West Felda Field with reference to the depositional models of Mural Limestone in Arizona, Glen Rose Limestone and Edwards Limestone in Texas, Abra Formation in Mexico. In this study, Mitchell-

Tapping and Mitchell-Tapping (2003) divided the Sunniland Formation into five widespread distinct units, proposed the Sunniland intertidal depositional model (Figure 6, A) with two major trends and developed 2-D mound type model for each trend (Figure 6, B, C).

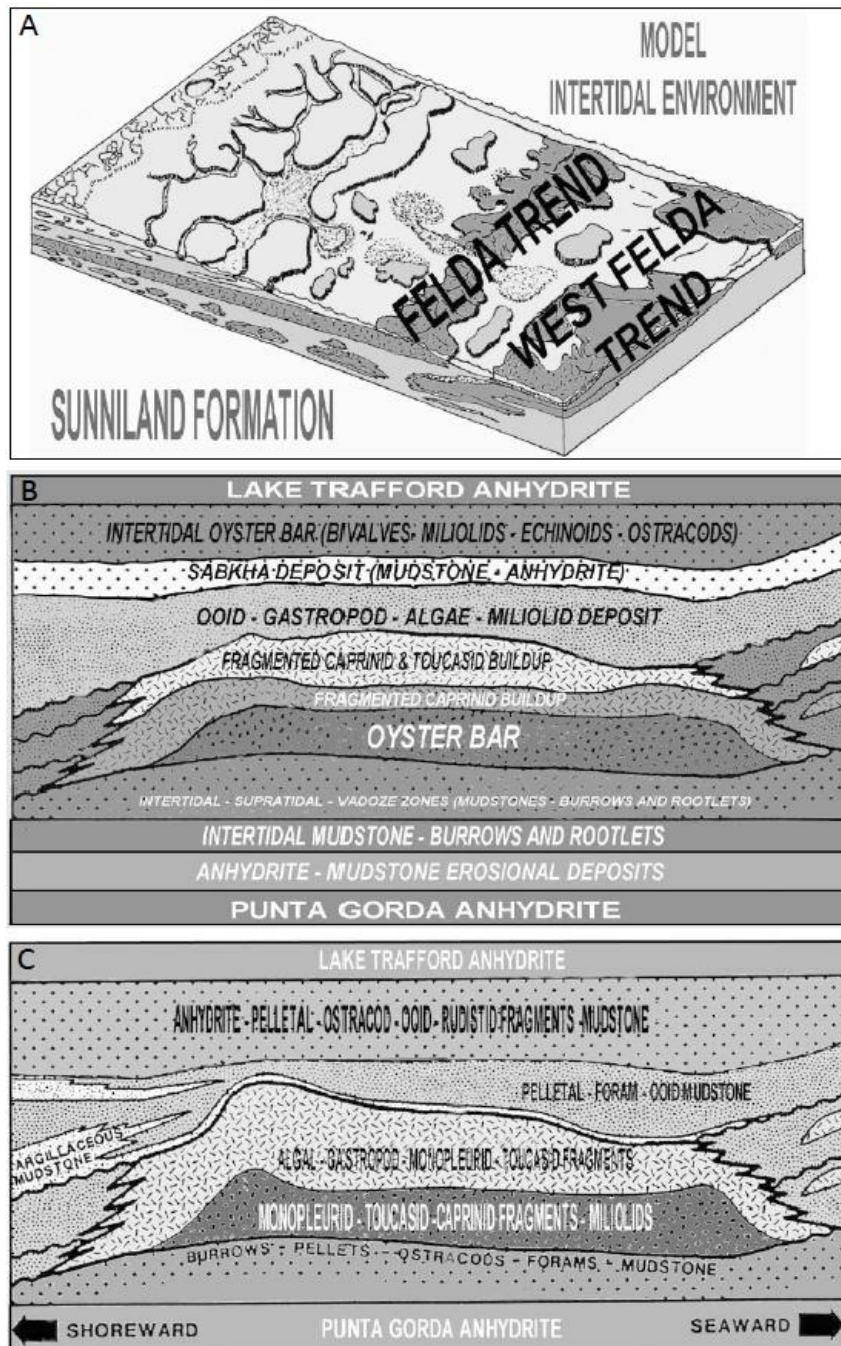


Figure 6: A. Model of the two major trends in the Sunniland Formation. B. West Felda Trend mound type model. C. Felda Trend mound type model (Mitchell-Tapping H. J., 2003).

Important work from Richards (1988) is the only high-resolution correlation of the Sunniland cyclicity and sequence stratigraphy that incorporates nearby fields to document how the shelf evolved near the area of Raccoon Point field. Figure 7 shows the location of wells and line of the section. This study outlined the deposition history of the Sunniland Formation in a series of sixteen parasequences and three sequences (see Figure 8) using the concepts of Vail et al (1984) and Van Wagoner (1985) and the principle of “keep up” and “catch up” from Kendall and Schlager (1981). Richards investigated the shoreline-to-outer shelf transect across the South Florida Basin, thereby allowing for the development of facies distribution maps to document the regional depositional history. The techniques used in my study are closely modeled after the work of Richards (1988).

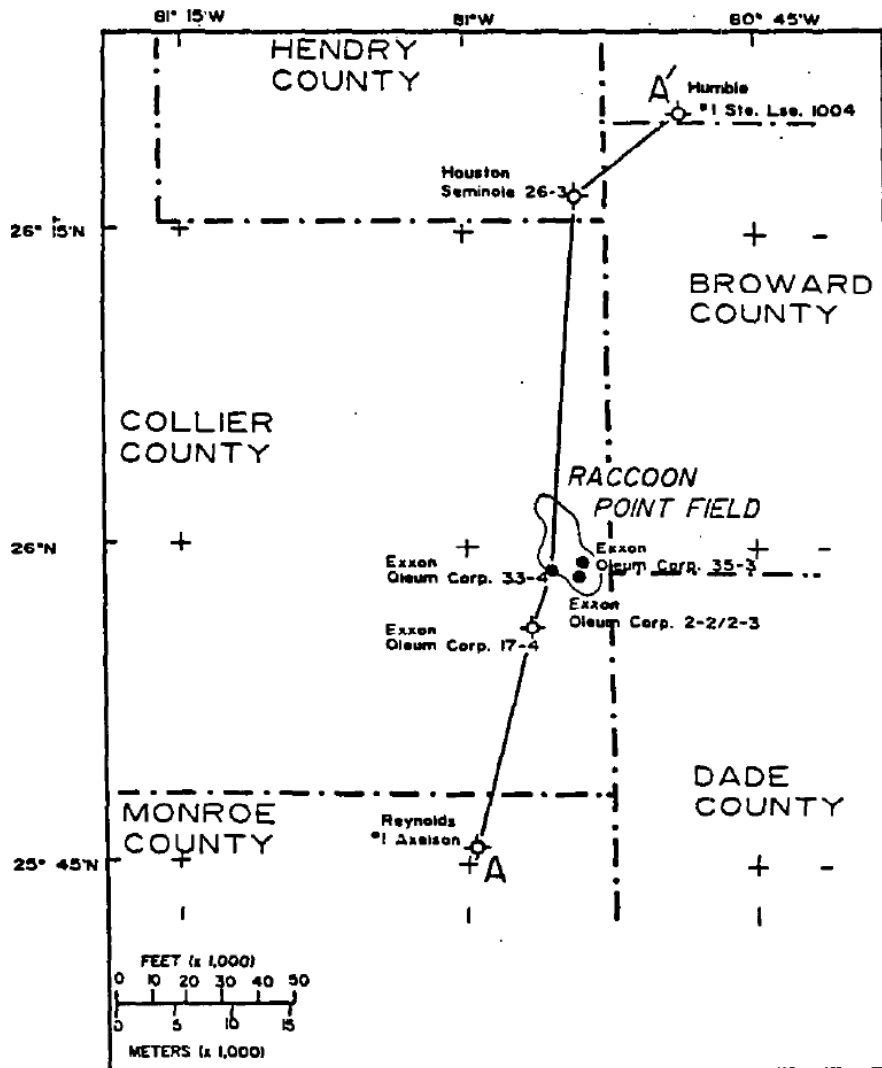


Figure 7: Map of Richards (1988)'s Study Area showing location of wells and regional cross-section A-A'.

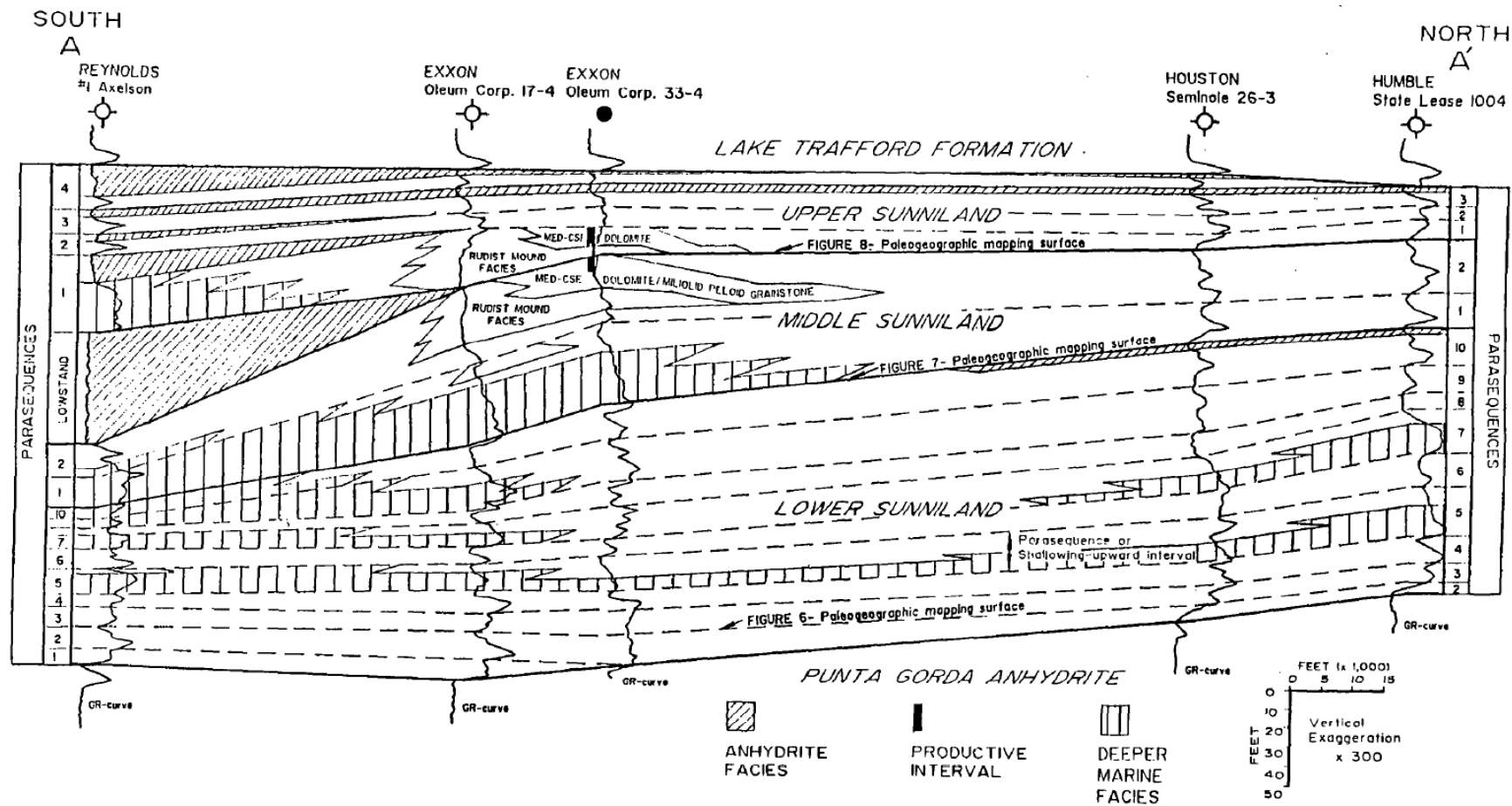


Figure 8: Cross-section A-A' showing correlations and distribution of anhydrite, rudist bioherms, and reservoir rock by Richards (1988). See Figure 7 for location of cross-section A-A'.

The U.S. Geological Survey (USGS) provided investigations on petroleum source rock potential of the Florida Peninsula (Palacas, 1984). In this study, detailed crude-oil-source correlations indicate that the algal-saprogenic, organic-rich argillaceous limestone in the lower Sunniland Limestone, particularly the down-dip basinal facies are the probable major source of upper Sunniland oil. The 1995 USGS National Oil and Gas Play-based Assessment of the South Florida Basin (Pollastro, 1995) delineated six conventional hydrocarbon plays in the South Florida Basin of Province 50 with only the Upper Sunniland Tidal Shoal Oil play (5001) and the Lower Sunniland Fractured “Dark Carbonate” Oil play (5002) as confirmed plays. Pollastro and Viger (1998) updated the maps of South Florida Basin structural uplifts, known Sunniland fields, and the boundaries of six plays based on the 1995 report. Pollastro et al. (2000) re-evaluated the hydrocarbon potential of the South Florida Basin using the total-petroleum-system-assessment-unit method and estimated a total of 702 MMBOE undiscovered oil and gas for the South Florida Basin, as compared to a total of about 377 MMBOE from the 1995 USGS assessment.

Due to the absence of Sunniland outcrops and the limitation on offshore drilling activity, no work has tied both outcrop and subsurface studies to document the shelf-to-basin transect across the South Florida Basin. However, Phelps’s (2011) work on the Comanche Platform evolution has established key regional stratigraphic relationships in the Northern Gulf of Mexico, enabling the development of a predictive model for future field placement in the Eastern Gulf of Mexico. In addition, recent Albian patch-reef outcrop studies in the Pipe Creek of Texas (Kerans and Zahm) and the Grassy Hill and Paul Spur of Arizona (Figure 9; Aisner and Kerans, 2010) provided a wealth of information regarding the changing biota, sea level, ocean chemistry, and climate of the Albian in the Northern Gulf of Mexico. These studies can bring new insights in understanding the paleo-reef ecology, morphodynamics of the tidal shoal complex; and helped unravel the temporal and spatial variability of the Florida shelf-margin barrier reef during the Albian deposition.

Likewise, the depositional models of Bebout and Loucks (1974) have been useful for understanding initial observations during data collection of this study. Rapid growth of *toucasid-caprinid* bioherms and progradational cyclic subtidal packstones to grainstones are characteristics of the lower Albian patch-reef deposition during the early highstand at

Red Bluff Creek, Texas (Kerans and Zahm) and SE Arizona (Paul Spur and Grassy Hill) (Aisner and Kerans, 2010). In South Florida, the stacked intertidal cycles and patch-reef growth patterns are similar to the observations from the Pipe Creek outcrop, the Grassy Hill and Paul Spur outcrops (Figure 9), both of which depict a distally steepened ramp profile. Thus, the depositional models generated from these outcrop studies can help interpret scales of facies variability, and predict stratigraphic positions of key reservoir facies of the Sunniland Fm. Yet, in South Florida, the scarcity of corals within the caprinid buildups, the more landward position, and the proximity to equator may suggest a slightly harsher, warmer condition. In all, no single static model will account for every facies variation; however, these models offer broad guidelines to facies deposition in shallow-water Sunniland carbonates.

South

North

Paul Spur
(patch-reef)

Grassy Hill
(ramp interior)

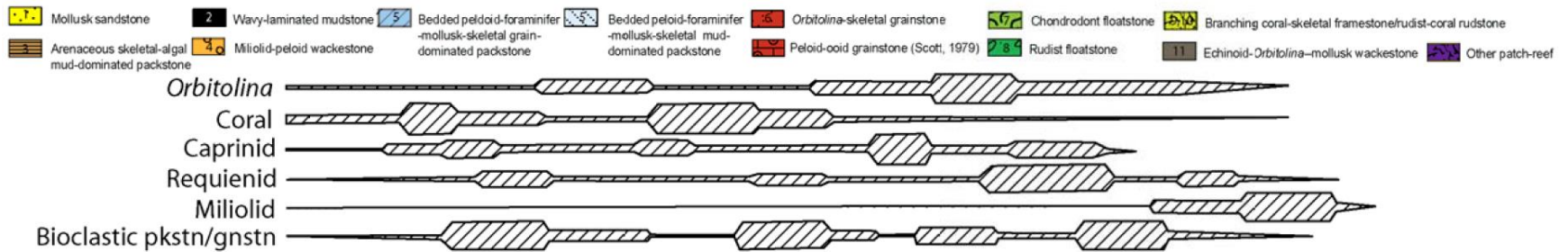
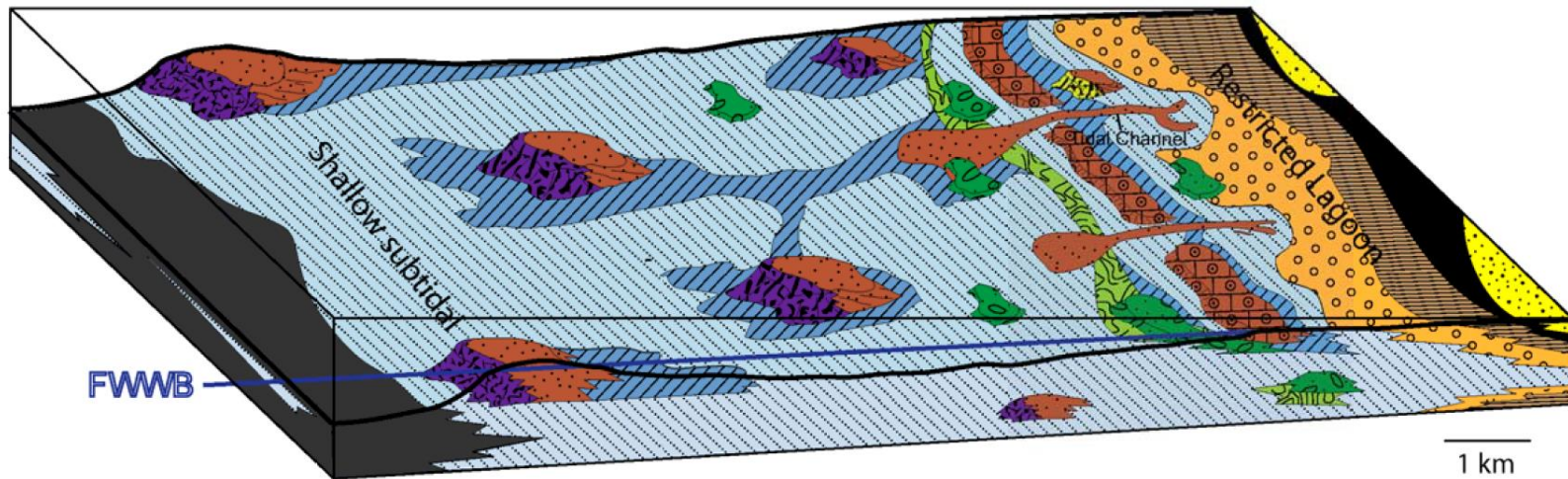


Figure 9: Facies and interpreted depositional environments of the Mural Limestone ramp interior at the Grassy Hill and Paul Spur patch-reef study areas, southeastern Arizona. The conceptual model spans a 15 km transect that represents a depositional dip profile from north to south. Lateral facies associations are based on vertical relationships in measured sections. The Grassy Hill facies are interpreted to be deposited in a marginal marine/restricted lagoon, ooid shoal and shallow-water subtidal ramp interior setting. Large coral patch-reefs (~30 m thick), such as the one studied at the Paul Spur locality, are constrained to the shallow subtidal only. Smaller (~6 m) coral patch-reefs are present updip at the Grassy Hill locality. Caprinid-requienid buildups with moderate (up to 5 m) relief are prevalent in the shallow subtidal setting and smaller scale caprinid-requienid buildups (1-2 m) are associated with restricted marine miliolid-peloid wackestone facies. (Aisner & Kerans, 2011).

Methods and Data

In order to characterize the Sunniland Formation, four steps were taken. First, characterization of carbonate facies and interpretation depositional environments was undertaken using core and thin-section data and comparison with previous studies described above. Then, vertical facies successions were examined in terms of one-dimensional facies stacking patterns and merged with log data. Subsequently, correlation between wells was carried out following cycle and sequence hierarchy interpreted from the stacking pattern analysis. Once constructed, the detailed study area was compared to the basin-wide stratigraphic models that are constrained by Felda and Raccoon Point fields.

Cores, facies photos, petrographic images and digitized wireline logs are the basic data of this study. Eight cores totaling approximately 1000 feet from the Felda Sunniland Unit (FSU) were described and thin-section samples were taken from seven of them in order to further identify grain types, pore types, and skeletal allochems. All eight core descriptions and their associated symbol key are included in Appendix A. Dunham's (1962) depositional texture classification was used for depositional fabric identification. Fifty-two raster and gamma ray wireline logs penetrating the top of the Sunniland Formation and 16 logs penetrating the top of the Punta Gorda Fm are available for correlation in the study area. Industry seismic data are not available.

High-frequency cycle (fifth-order) tops were picked based on the principles outlined by Phelps (2011) in his study of the Comanche platform in south Texas: 1) upward decrease in mud within rock texture, 2) upward increase in hydrodynamic sedimentary structures, and grain size and sorting, 3) shallowing of peritidal biogenic and sedimentary structures, 4) change from horizontal, argillaceous *Planolites*-burrowed facies to vertical, *Thalassinoides*-burrowed. High-frequency cycle sets and high-frequency sequences (fourth-order) were identified using lithofacies proportions and cycle stacking patterns within vertical core profiles (Goldhammer et al., 1990; Mitchum and Van Wagoner, 1991; Kerans and Tinker, 1997).

Wireline logs spread along the line of section were used to constrain correlations between core and outcrop intervals. All logs along the cross section are datumed from the Lake Trafford Fm., a lithostratigraphic surface that is regionally extensive and presumed

to approximate a nearly horizontal depositional timeline. Established cycle and sequence tops were tied to the raster and gamma ray logs. The lithostratigraphic correlation of the study area depends on the observation of changing lithofacies proportion between successive high-frequency cycle sets (HFCs) and of changing faunal diversity. The detailed mapping of the Paul Spur, Grassy Hill, and Pipe Creek patch-reefs revealed a similar vertical stacking pattern and supports the lateral facies correlations made here, helping to unravel relationships between caprinid buildup, back-reef debris apron, and platform interior skeletal grainstone shoals. Richards (1988) Raccoon Point Field study within the Sunniland Trend has increased our understanding of platform carbonates on the field scale. The facies maps and basin-wide stratigraphic models are constrained by the sequence analysis of shelf-interior facies succession in the Felda Sunniland Unit (FSU), Raccoon Point field, and other Sunniland fields.

Lithofacies

INTRODUCTION

Six lithofacies associations (Table 1) represent the full Sunniland depositional system in south Florida. Lithofacies typifying each association are briefly described and interpreted with reference to previous studies.

Facies Associations	Facies Ref.		Facies Name
Sabkha-hypersaline lagoon	A		Nodular, mosaic anhydrite with dolomite lenses
Peritidal mudstone to grainstone	M	W	Bivalve mudstone/wackestone
	Ct. P	Ct. R	Intraclastic lime packstone/rudstone
	Rt. P		Rooted lime packstone
Flooded shelf shale	Arg. M		Argillaceous lime mudstone
Cyclic subtidal shelf wackestone-grainstone	Orb. P	Orb. W	<i>Orbitolina</i> -skeletal wackestone/packstone
	Mil. P	Mil. W	Miliolid-skeletal wackestone/packstone
Shelf-interior bioherm/biostrome	R. F		Rudist floatstone
	R. B		Rudist bafflestone
	R. R		Rudist rudstone
	Chon./Mon. F		Chondrodont/monopleurid floatstone
Molluscan grainstone shoreface/shoal	Orb. G		<i>Orbitolina</i> -bivalve grainstone
	Mil. G		Miliolid-skeletal grainstone
	Ooi. G		Peloid-oid grainstone

Table 1: Facies associations and facies names.

SABKHA-HYPERSALINE LAGOON

Facies A: Nodular, mosaic anhydrite with dolomite lenses

Anhydrite deposited in sabkha and salina commonly show extensive early diagenesis, so the interpretations on the initial depositional fabrics are often difficult. The anhydrite facies here features mosaic anhydrite or nodular anhydrite interfingering with laminated dolomite lenses. The presence of chicken-wire pattern (Figure 10 C) is commonly used as evidence of supratidal origin (Loucks and Longman, 1982). The centimeter-laminated dolomite lenses are also common and sometimes slightly burrowed. The thicker laminated dolomite lenses often accompanied with more burrows and thus suggesting a deepening of water depth.

Facies-A dominates all core of the Punta Gorda Formation within Sunniland trending band and extends basinward (Montgomery, 1987; Pollastro, 1995). This anhydrite is similar to that described by Loucks and Longman (1982) in the Ferry Lake Formation, which indicates a restricted, hypersaline, shallow-water subtidal environment. The general sedimentary structure and extensiveness of this facies indicates a broad, supratidal sabkha to hypersaline lagoonal environment (Loucks, 1985) and possibly barred from the open sea by shelf-margin rudist bank buildups near the Florida Escarpment. In addition, the deposition of laminated dolomite such as that observed at 11872 ft in well 31-2 may indicate a period of normal-salinity probably led by a break in the shelf margin barrier reef or periodic rise of the sea level.

The bedded nodular anhydrite capping the top of Sunniland Peloid-oid grainstone at well 31-2 may suggest exposure of the shoal and development of supratidal sabkha conditions (Loucks, 1985). While in the leeward side at well 15-3 and 35-4, the miliolid-peloid mudstone and fine-crystalline dolomite interfingers with sabkha anhydrites (Richards, 1988). This nodular anhydrite mudstone interbedded with massive anhydrite provides the seal for the Sunniland Formation (Feitz, 1976). Anhydrite increases upward with the progradation succession of restricted marine facies suggesting a sea-level fall; and resulted in a transition of facies eventually leading to the massive anhydrite deposition in the overlying Lake Trafford Fm. (Ferber, 1985).

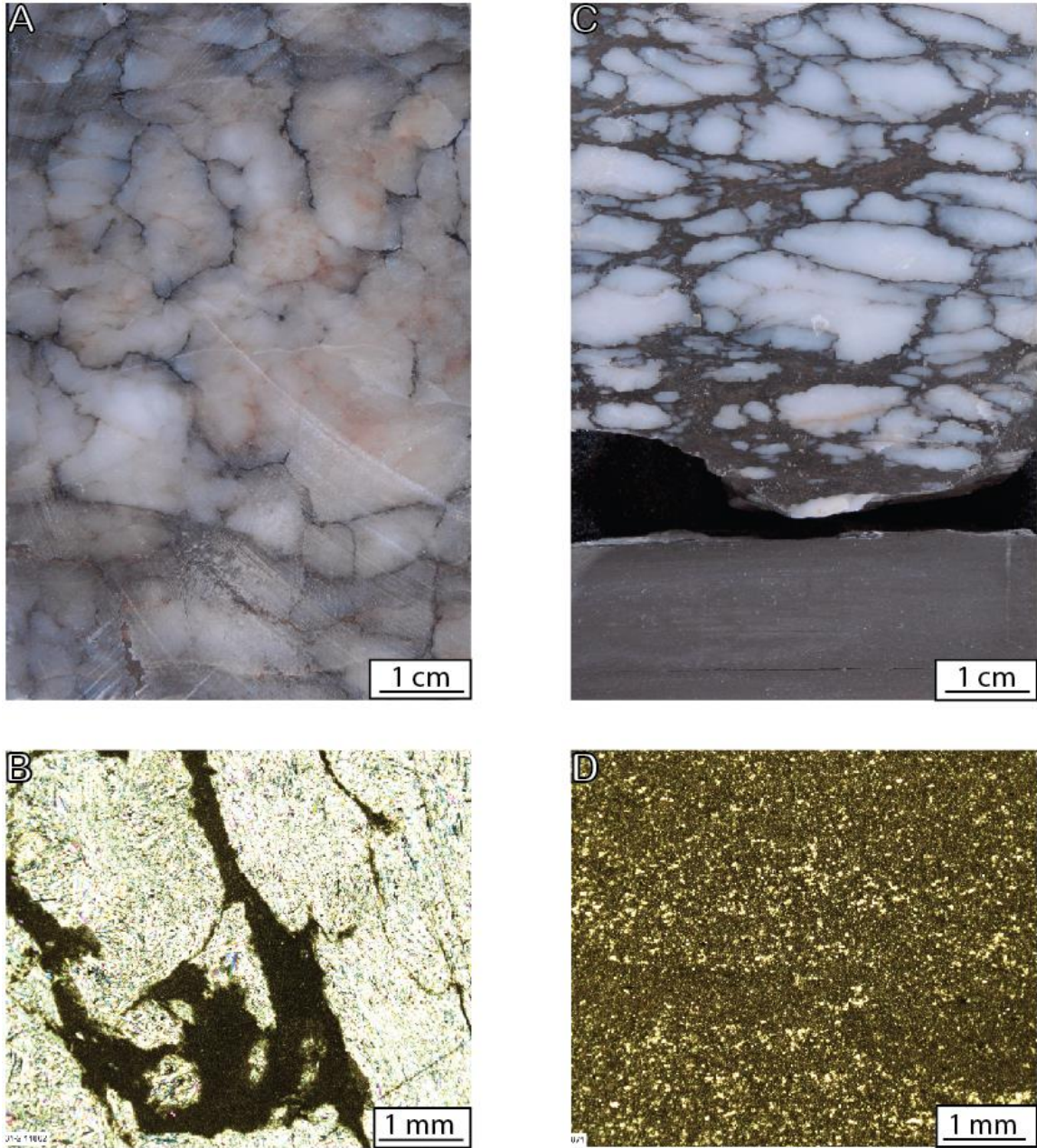


Figure 10: Anhydrites with dolomite lenses. (A) Mosaic anhydrites. Well 31-2 Depth=11,859 ft. (B) Photomicrograph of the anhydrite nodules displaying felted anhydrite crystals. The darker material is dolomite. Well 31-2. Depth=11,862 ft. (C) Well 31-2 Depth=11,872 ft Nodular anhydrite with chicken-wire pattern. (D) Photomicrograph of the laminated dolomite. Well 31-2. Depth=11871 ft.

PERITIDAL MUDSTONE TO GRAINSTONE

Tidal, storm-influenced sedimentary structures and evidence of periodic subaerial exposure in a peritidal-supratidal setting typify this carbonate facies assemblage.

Facies Ct. P: Intraclastic Lime Packstone/Rudstone

Directly overlying the Punta Gorda Anhydrite, clasts of lime packstone comprise intercalated upward-coarsening gravel, intraclastic rudstone limestone, and felted anhydrite nodules in the mollusk wackestone matrix (Figure 11). Clasts are poorly-sorted and commonly coated with bladed calcite rim cement surrounded by sparry cement. In some cases, compaction along the contact of some mud clasts suggests that the mud had not lithified at the time compaction occurred. In addition, the presence of large basal intraclasts (up to 4 cm) may represent basal channel deposits and dissected intertidal deposits (Richards, 1988).

Facies Rt. P: Rooted lime packstone

The rooted lime packstone features abundant rhizcretions (R) (Figure 12a,c) and desiccation clasts in a matrix of mollusc mudstone and wackestone (Figure 12b, d). Sedimentary structures include mudcracks, fenestrae, algal laminations, churned intervals, and dolomite crusts. This facies represents brief to longer periods of subaerial exposure marking the tops of upward shallowing cycles. The presence of root tubes and other subaerial exposure features indicate a lower intertidal to supratidal environment.

Facies M/W: Mollusk mudstone/wackestone

The mollusc lime mudstone/wackestone is commonly the background facies of the tidal-, storm-influenced, subaerial exposure sedimentary structures (Figure 12b, d). Thus, it is prevalent at the base of the Sunniland Fm., intercalated with intraclastic lime packstone/rudstone, and rooted packstone. Carbonate allochems include rare miliolids, echinoids, pelecypods, ostracods, serpulids, and unidentified thin-shelled mollusc fragments. The sparse presence of miliolids and scarcity of other mollusc fauna may suggest a harsher marine condition. The interval with few clasts and sparse mollusc fragments particularly indicates a period of slow deposition during a fluctuating transgressive sea in a normal to slightly restricted, low- to moderate-energy conditions.

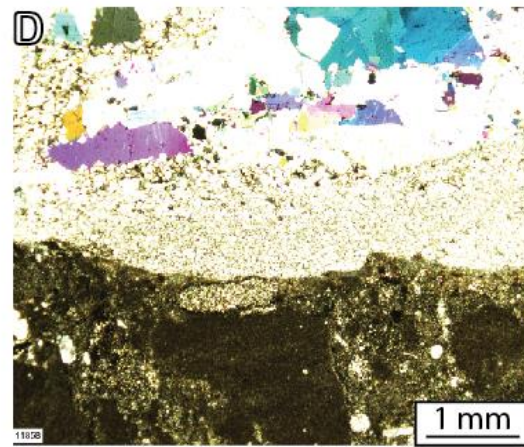
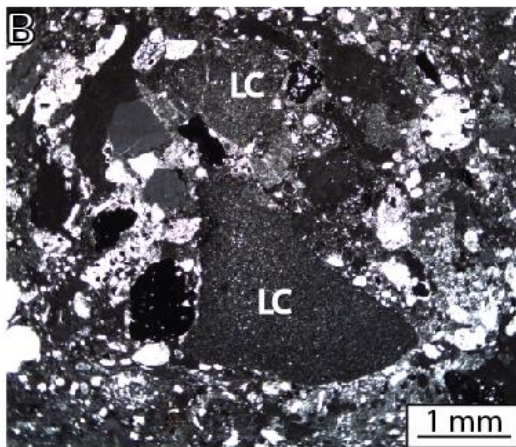
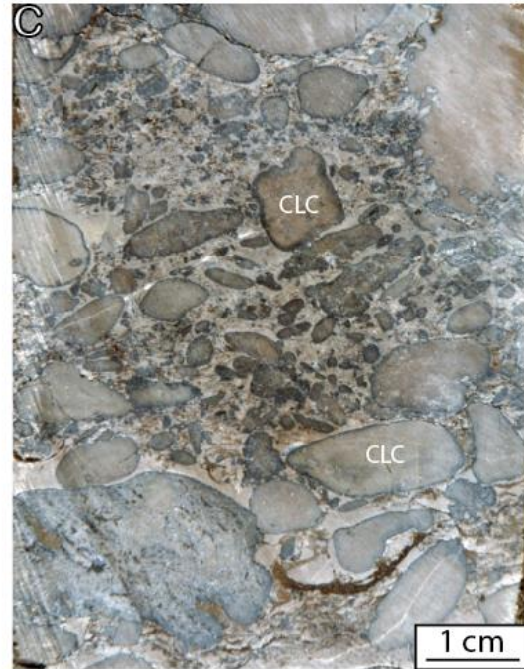


Figure 11: Intraclastic lime rudstone. (A) Intraclast-rich lime packstone deposited in tidal flat environment. Compaction along the contact of some mud clasts suggest that the mud had not lithified. Well 31-2 Depth=11,857 ft. (B) Lithoclast (LC) lime packstone. Well 31-2. Depth=11,858 ft. (C) Lithoclast lime packstone. Coated lithoclast (CLC) Well 33-2 Depth=11,652 ft. (D) A dolomitized intraclast. Well 31-2. Depth=11,858 ft.

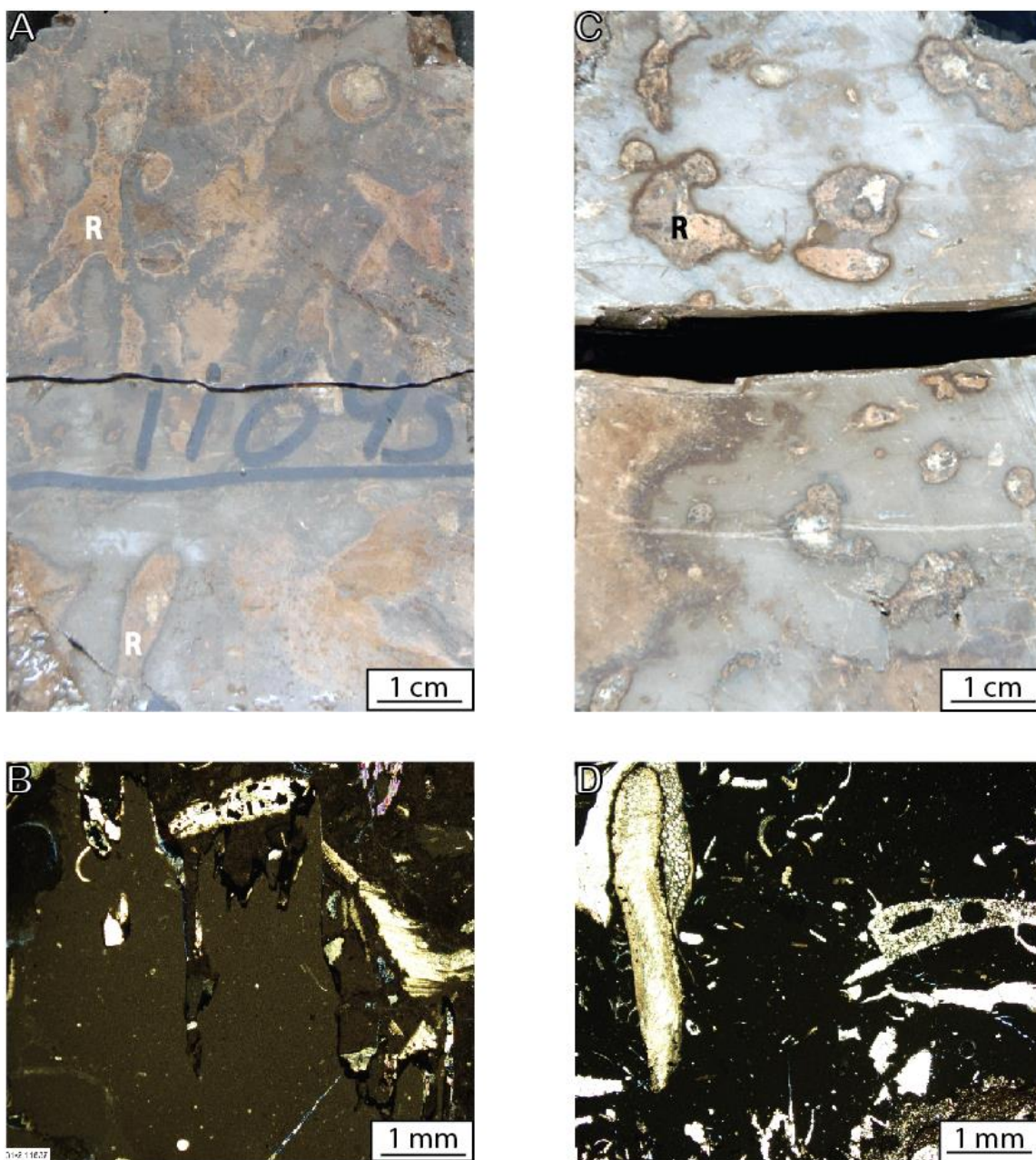


Figure 12: Rooted lime packstone (A) Plant roots in lime mudstone. Rhizoconcretions (R) Well 31-2 Depth=11,845 ft. (B) Pressure solution seams. Well 31-2. Depth=11,837 ft. (C) Roots in lime mudstone. Rhizoconcretions (R) Well 33-2 Depth=11645 ft. (D) Tidal flat wackestone. Well 33-2. Depth=11,644 ft.

MUDSTONE/WACKESTONE

Facies Arg. M: Argillaceous mudstone

Medium-dark gray mudstone features wispy algal laminations fabric with abundant silt-sized particles and few skeletal fauna. The mudstone is occasionally fractured, and frequently produces a petroliferous odor from fresh surfaces (Mitchell-Tapping, 2003). Burrows are locally common. The facies dominates the lower section of the Sunniland Formation with a basinward increase in thickness (Lloyd and Applegate, 1985) and thus creates a consistent wireline-log signal over all wells in this and all other studies. Organic-rich argillaceous limestone are the probable major source of upper Sunniland oil (Palacas, 1984). The deposition of this argillaceous lime mudstone indicates a significant shift to a deeper marine condition on a flooded shelf (Phelps, 2011).

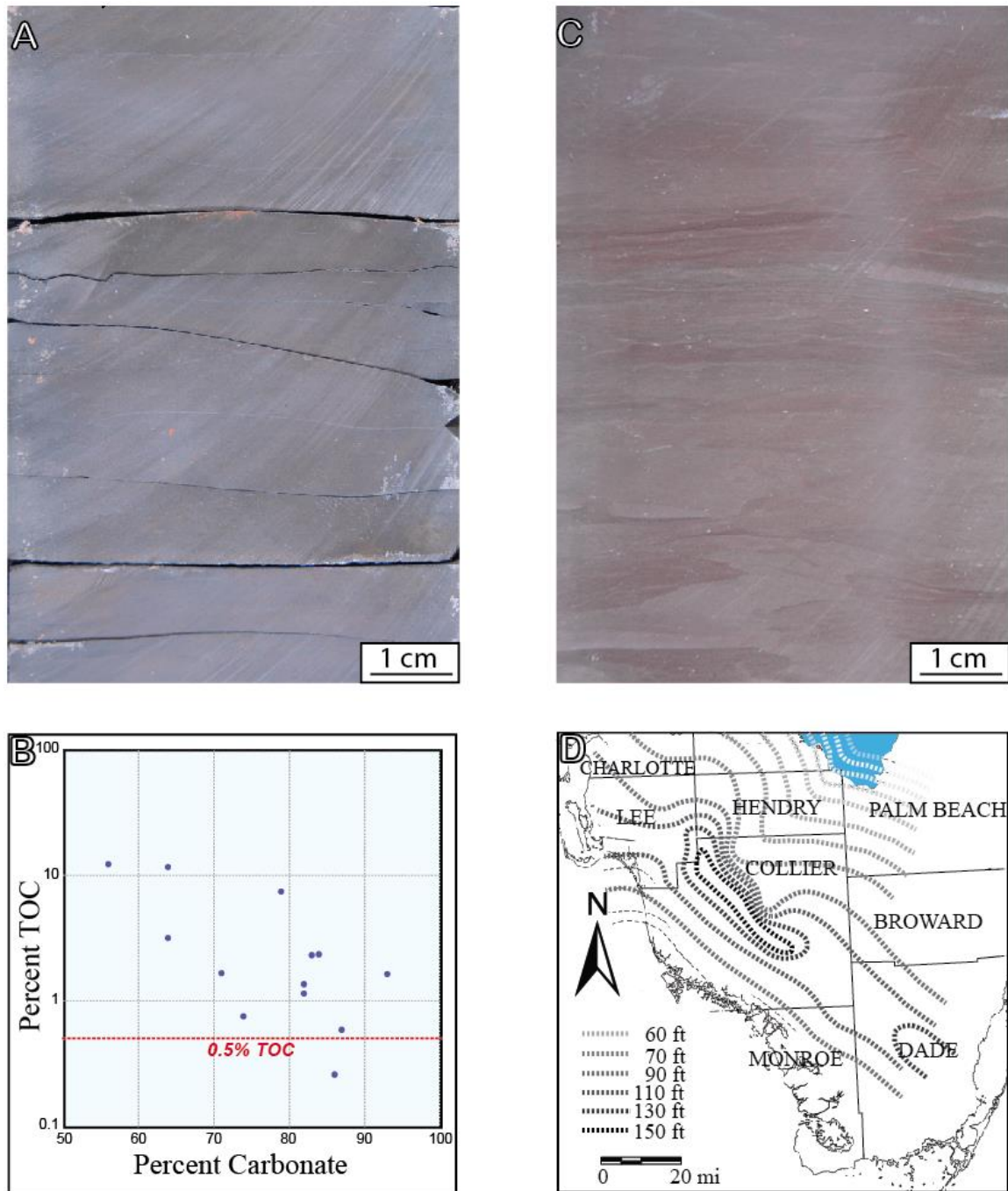


Figure 13: Argillaceous mudstone. (A) Argillaceous lime mudstone. Well 28-3 Depth=11,573 ft. (B) TOC % vs Carbonate %. Argillaceous lime mudstone. Marginal mature. Algal-saprogenic organic material. (Palacas, 1984). (C) Laminated/burrowed dolomudstones. Well 28-3 Depth=11,550 ft. (D) Isopach of lowermost argillaceous lime units. (Applegate and Pontigo, 1984).

CYCLIC SUBTIDAL SHELF WACKESTONE-PACKSTONE

Lithofacies in this assemblage contain assorted allochems, varied fauna, and range from wackestone, to mud- and grain-dominated packstone, to grainstone. *Orbitolina* facies transgressed across the ramp during flooding events, whereas miliolids were most abundant in the more restricted condition (Phelps, 2011).

Facies Orb. W/P: Orbitolina-skeletal wackestone/packstone

Orbitolina-skeletal wackestone is comprised of lime mud with *Orbitolina* foraminifers, gastropods, and non-descript skeletal hash (Figure 14a, c). From petrographic examination, *Orbitolina* exhibit a low aspect ratio (disk-like) (Figure 14b, d); Diagenesis has alternated carbonate mud with massive patchy dolomite and filled the dissolved allochems with baroque dolomite (Figure 14b). The *Orbitolina*-skeletal wackestone is overlain by rudist floatstone at the base of the reef core of well AL 31-2 and by rudist rudstone in West Felda fields. It grades laterally leeward into *Orbitolina*-skeletal packstone/grainstone to form a shoal bar or split through storm or wave transportation. The abundance of carbonate mud and disk-like morphology of *Orbitolina* are indicative of open-marine subtidal shoal. The diverse marine fauna suggest well-oxygenated and well-lit normal marine conditions. The depositional conditions are commonly associated with a stable substrate for patch-reef nucleation (Scholle, 1983) and therefore created a hospitable environment for the solitary rudist to thrive and aggregate into shelf-interior rudist bioherms observed from the S-4 interval of well 31-2. The massive, millimeter-sized, horizontally aligned molds observed on the core surface are likely after *Orbitolina*.

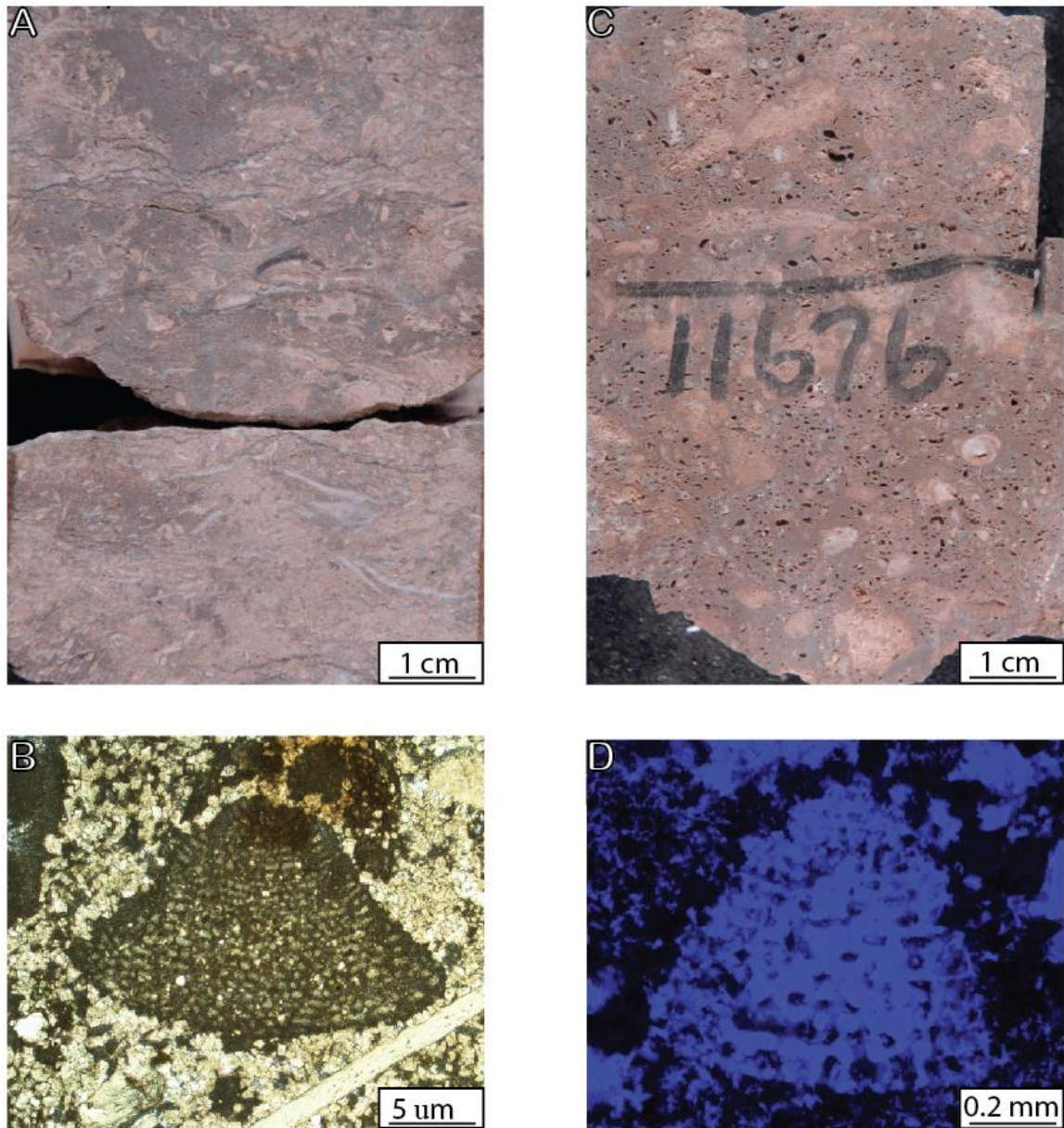


Figure 14: *Orbitolina*-skeletal wackestone/packstone. (A) and (C) Core slabs showing *Orbitolina*-skeletal packstone from Well 29-3 Depth=11491 ft and Well 31-2 Depth=11677 ft. (B) Photomicrograph showing *Orbitolina* from Well 31-2 Depth=11677 ft. (C) Photomicrograph showing micropores within *Orbitolina* under UV light.

Facies Mil. W/P: Miliolid-skeletal wackestone/packstone

The miliolid-skeletal wackestone/packstone forms massive rarely- stratified beds with fine-medium sand-sized grains. It is the most common depositional fabric observed from core samples in the S-4, S-5 intervals at the Sunoco Felda field. Miliolid-skeletal packstone is primarily composed of miliolids, peloids, and large gastropods but transported rudist fragments and other mollusc shells also occur. Miliolids have porcelaneous shell walls that appear white in core surface. Peloids are more common in the grain-dominated packstone fabric. Miliolid-skeletal wackestone/packstone is occasionally associated with thin-medium beds of toucasid-chondrodonta-monopleurid floatstone and intercalated with burrowed mudstone. Transported monopleurids commonly occur in the transitional lagoon-tidal flat area around colonies of chondrodontids, particularly between and behind the caprinid patch reef in a protected (leeward) shallow-water area with elevated salinity (Ferber, 1985). The high abundance of miliolids, low diversity of marine fauna, and the presence of *Thallasinoides* burrows support a low-energy, restricted subtidal environment.

Miliolid-skeletal wackestone/packstone commonly coarsens upward to miliolid-skeletal grainstone and overlies the burrowed mudstone and grades landward into the extensive beach deposits observed from the middle section at well 35-4. During Lower Cretaceous time, similar facies commonly indicate a restricted inner-ramp environment in the Pearsall Formation in Texas (Loucks, 1977), the Shuiaba Formation in the Middle East (Alsharan, 1995; Hillgartner et al., 2003), and the Mural Limestone in Southeast Arizona (Aisner and Kerans, 2010).

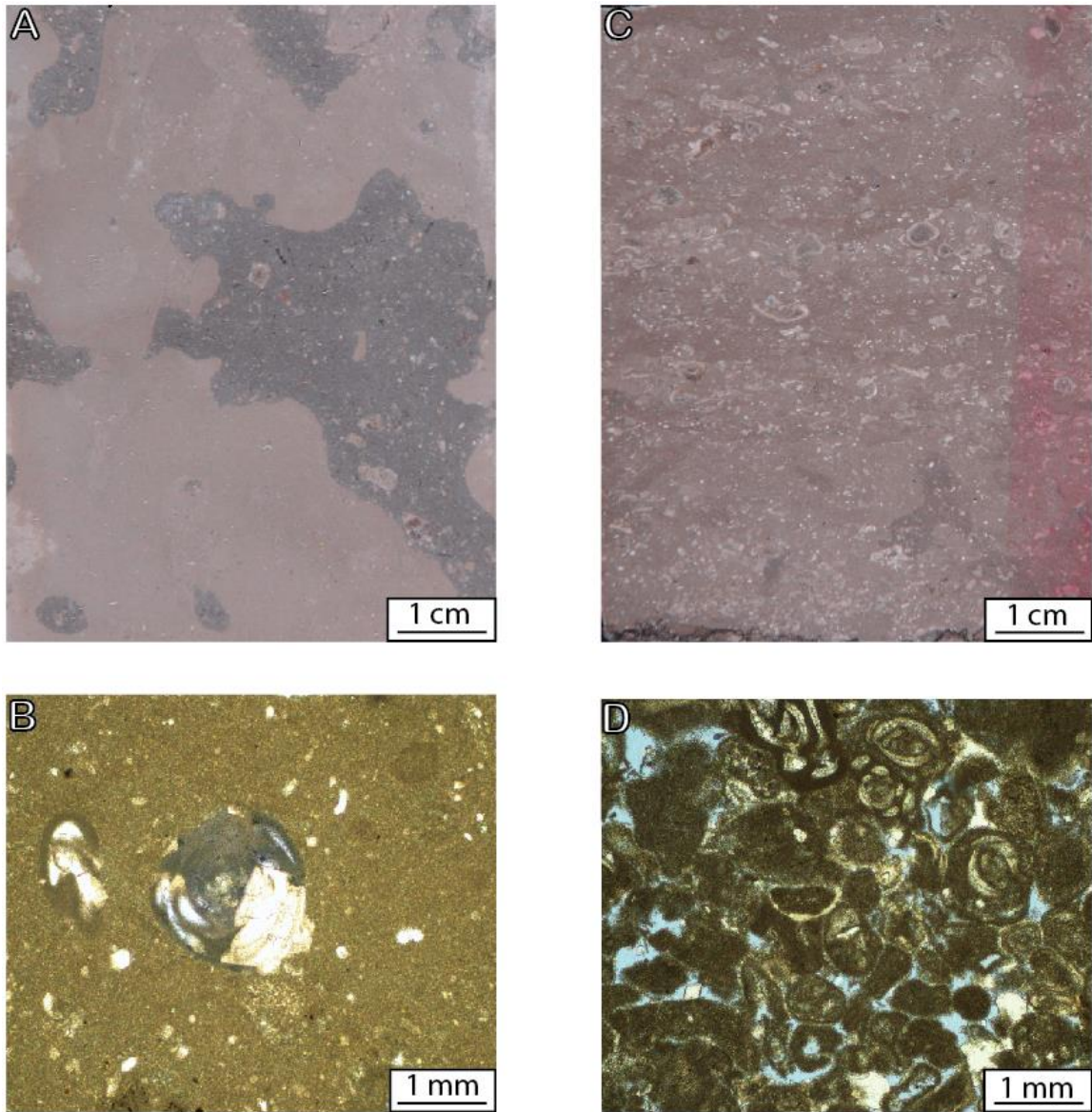


Figure 15: Miliolid-skeletal wackestone/packstone. (A) Core slab and (B) Photomicrograph showing burrowed miliolid-skeletal wackestone from Well 27-3 Depth=11475 ft. (C) Core slab and (D) photomicrograph showing miliolid-skeletal packstone from Well 28-3 Depth=11466 ft.

SHELF-INTERIOR BIOHERM/BIOSTROME

The high density of rudist bivalves typifies Albian shelf-interior bioherm/biostrome. Rudists are massively shelled, solitary and gregarious, inequivalve, suspension-feeding, epifaunal bivalves that lived on the margins of the Tethyan Ocean and adjacent areas from the end of Jurassic until the end of Cretaceous (Riccardo and Dario, 1995). The simplified rudist classification by Riccardo and Dario contains six main rudist families, and Caprinidae (Caprinids), Requiieniidae (Toucasids), Caprotinidae (Monopleurids) and radiolitids occur in this study.

Facies R. B: Rudist bafflestone

This dolomitized rudist bafflestone constructed the 50-ft thick mound community. It comprises massive whole tests of caprinids up to 5 cm in diameter. Borings on the rudist skeleton are uncommon. Petrographic evidence shows the medium-to-coarse crystalline dolomite (Figure 29) crystal size with little recognizable biogenic debris. Rudist bafflestone exhibits sharp contacts with the overlying rudist floatstone. In general, in contrast to toucasids, caprinids are generally associated with higher energy. Gregarious caprinids community serves as baffles to moderate-wave activity trapping skeletal fragments and lime mud, which reciprocally serves as stable substrate for more caprinids to dwell. This rudist bafflestone represents the active reef-growth catching up with the rising sea level to construct strata of positive relief above the surrounding lithofacies. The positive relief may provide sheltered, relatively low-energy areas for smaller toucasids to occupy (Loucks, 1985). Rudist bafflestone overlies *Orbitolina*-skeletal wackestone, underlies rudist floatstone at well 31-2 and grade laterally into debris apron grainstones by constant wave, tide and periodical storm reworking.

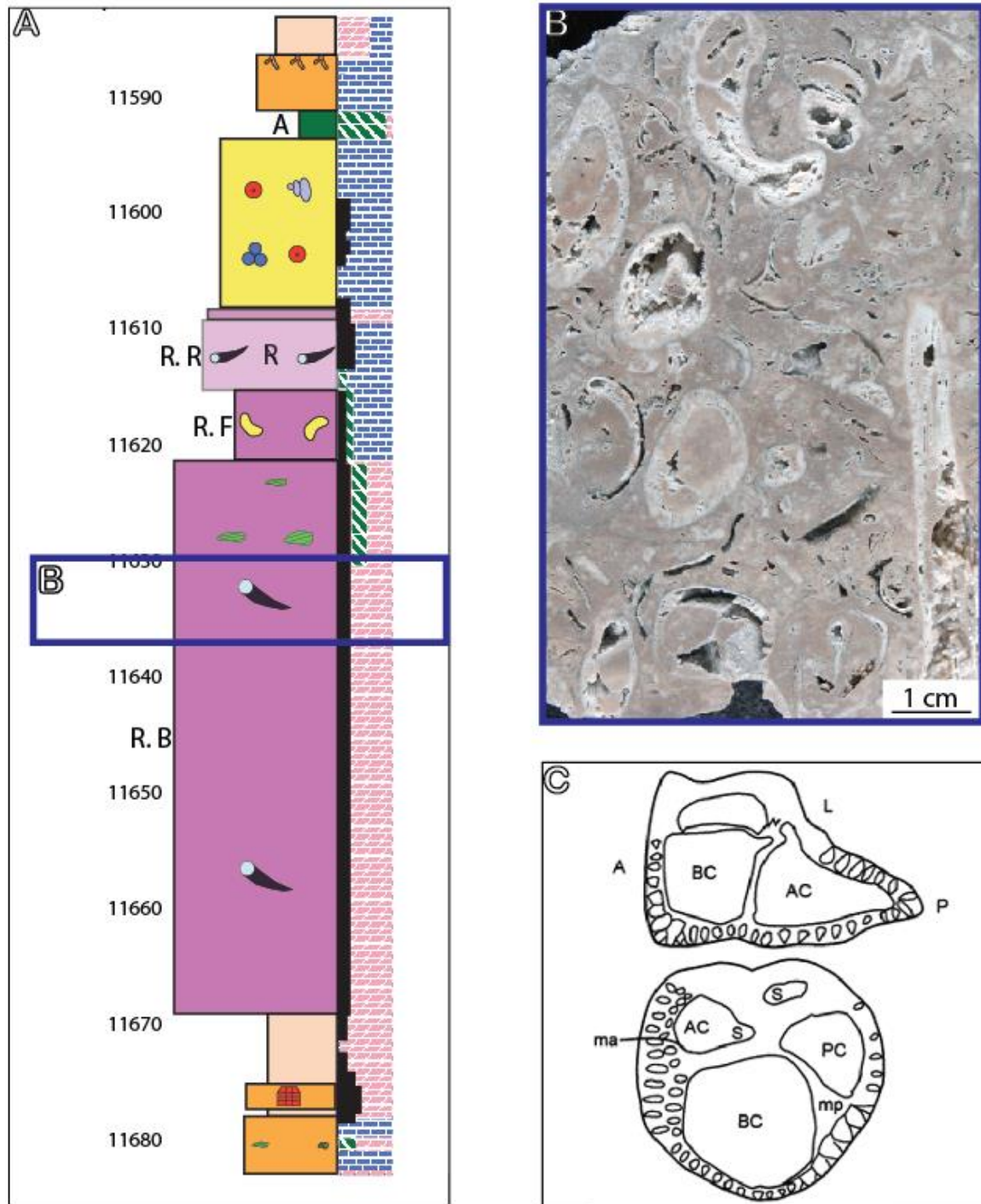


Figure 16: Rudist bafflestone. (A) Well 31-2 core description. (B) Rudist bafflestone. Well 31-2 Depth=11631 ft. (C) Main shell features of a caprinid. (A=anterior, P=posterior, S=socket, L=ligament, AC=accessory cavity, PC=posterior cavity. mp=myophore) (Scott R. W., 2002).

Facies R. F: Rudist floatstone

Light gray rudist floatstone comprises toucasids, caprinid, and minor radiolitids in a peloid-rich wackestone and packstone matrix. Matrix allochems include *Orbitolina* and peloids. The relative abundance of smaller toucasids and the scarcity of encrusting phototrophic organisms and presence of *Orbitolina* indicate a deeper or sheltered, low-energy setting. This facies overlies the massive rudist bafflestone. It may indicate a period of further sea-level rise and therefore may correlate to the packstone facies at West Felda Fields.

Facies R. R: Rudist rudstone

Rudist rudstone is comprised of large fragmental caprinids and massive nondescript lithoclastic bivalve fragments. Petrographic evidence indicates that bivalve fragments underwent meteoric dissolution, and commonly coated with microbial encrusting organism such as *Lithocodium/Bacinella*, which in turn are bored. This provides evidence for a shallow well-lit condition (Dupraz and Strasser, 2002). The abundance of dissolved bivalve fragments and the presence of *Lithocodium/Bacinella* and the absence of carbonate mud are characteristic of a high-energy shoaling condition. Once the patch reef grew into such condition, it is episodically affected by storms and surrounded by skeletal debris aprons developing along the shallow-reef margins (Loucks, 1985). This facies overlies rudist floatstone and overlain by peloid-oid grainstone at well 31-2 near Corkscrew field and extends landward and grade laterally into skeletal grainstone at West Felda field and it might be further transported landward by storms and tides to the tidal-shoal complex at Sunoco Felda field.

Facies Mon. Chon. F: Monopleurid/chondrodont floatstone

The lack of petrographic evidence of *Orbitolina* and the absence of caprinid fragments distinguish the thin-layers of chondrodonta floatstone observed basinward in a more restricted environment from the rudist floatstone observed at Al 31-2. In Sunoco Felda and Mid Felda, the horizontally oriented chondrodonts are commonly directly overlain by transported or in-situ monopleurids as well as toucasids. The presence of abundant miliolids in chondrodont floatstone indicate a low-energy, more restricted environment below fair-weather wave base. In Texas, this facies is found in the middle

ramp Pine Island Shale and upper Bexar Shale intervals, forming widespread correlative biostromes (Loucks, 1977). It connects to the OAE 1a, 1b (Hull, 2011; Phelps, 2011) in Texas and likely marks the onset reestablishment of carbonate factory from a stressed environment created by OAE 1-B in the South Florida Basin.

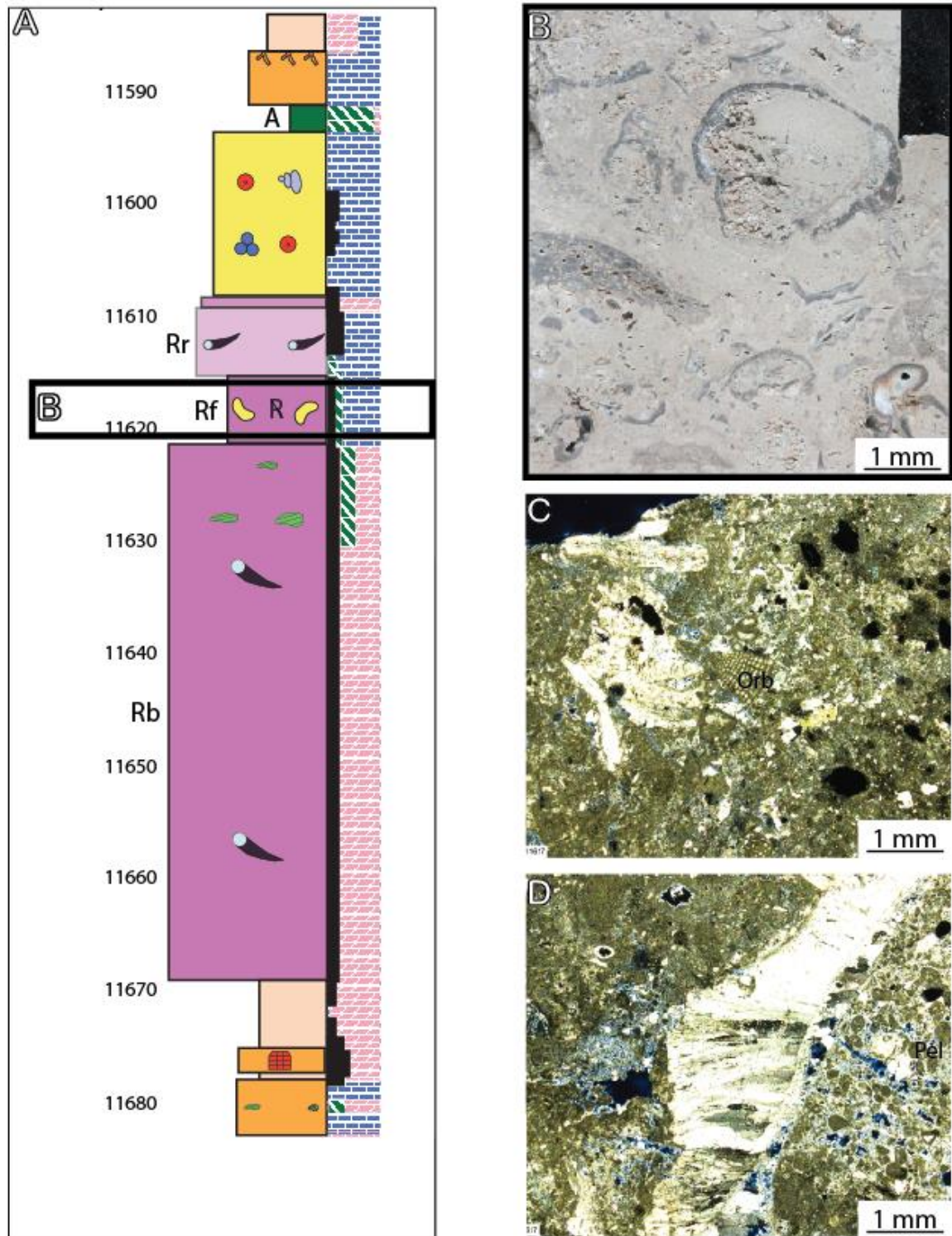


Figure 17: Rudist floatstone. (A) Well 31-2 core description. (B) Well 31-2 Depth=11617 ft. (C) and (D) photomicrographs showing rudist floatstone from Well 31-2 Depth=11617 ft. *Orbitolina* (Orb). Peloid (Pel).

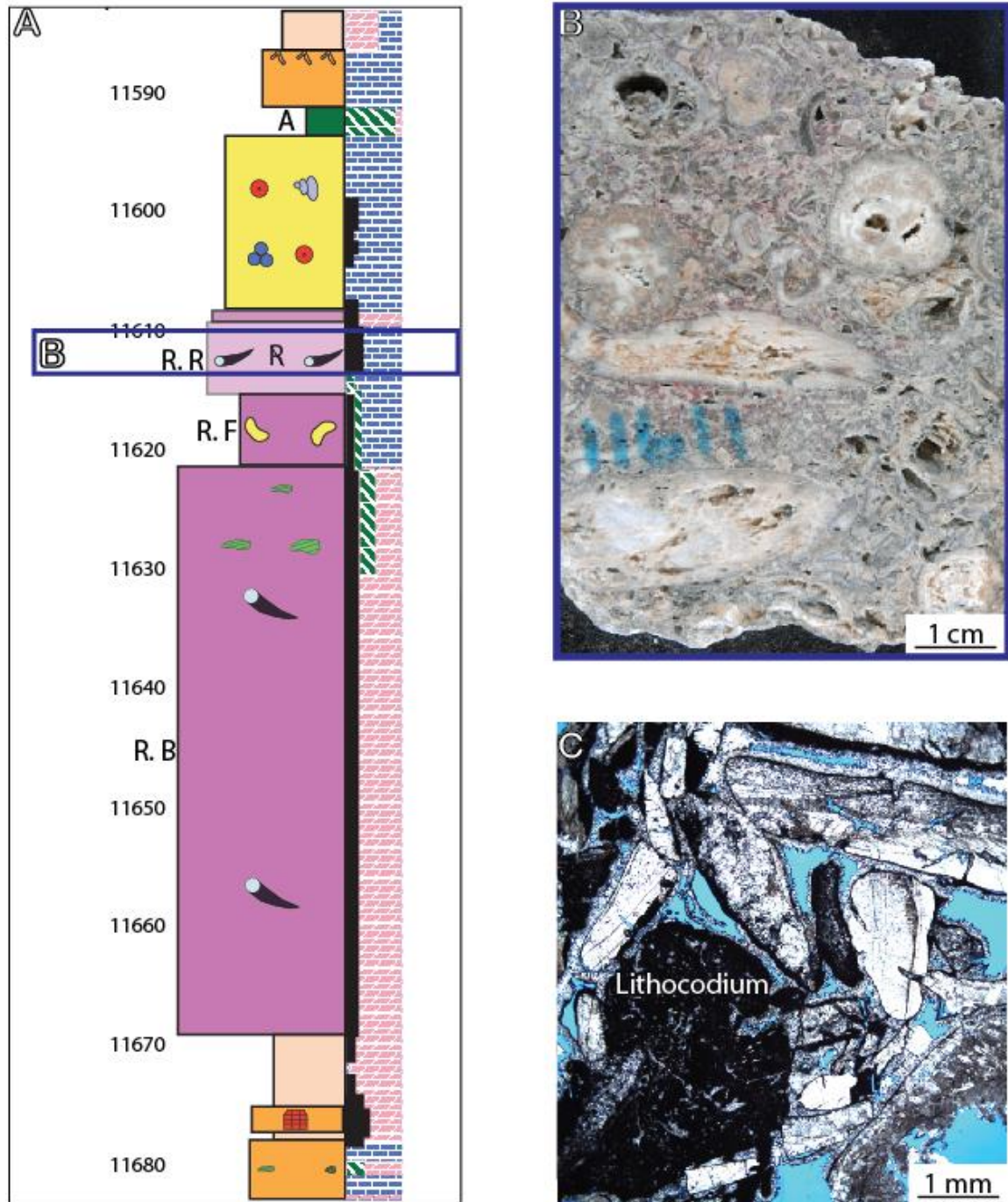


Figure 18: Rudist rudstone. (A) Showing core description of well 31-2. (B) Core slab showing rudist rudstone from well 31-2 Depth=11611 ft. (C) photomicrograph showing rudist fragments coated with *Lithocodium*.

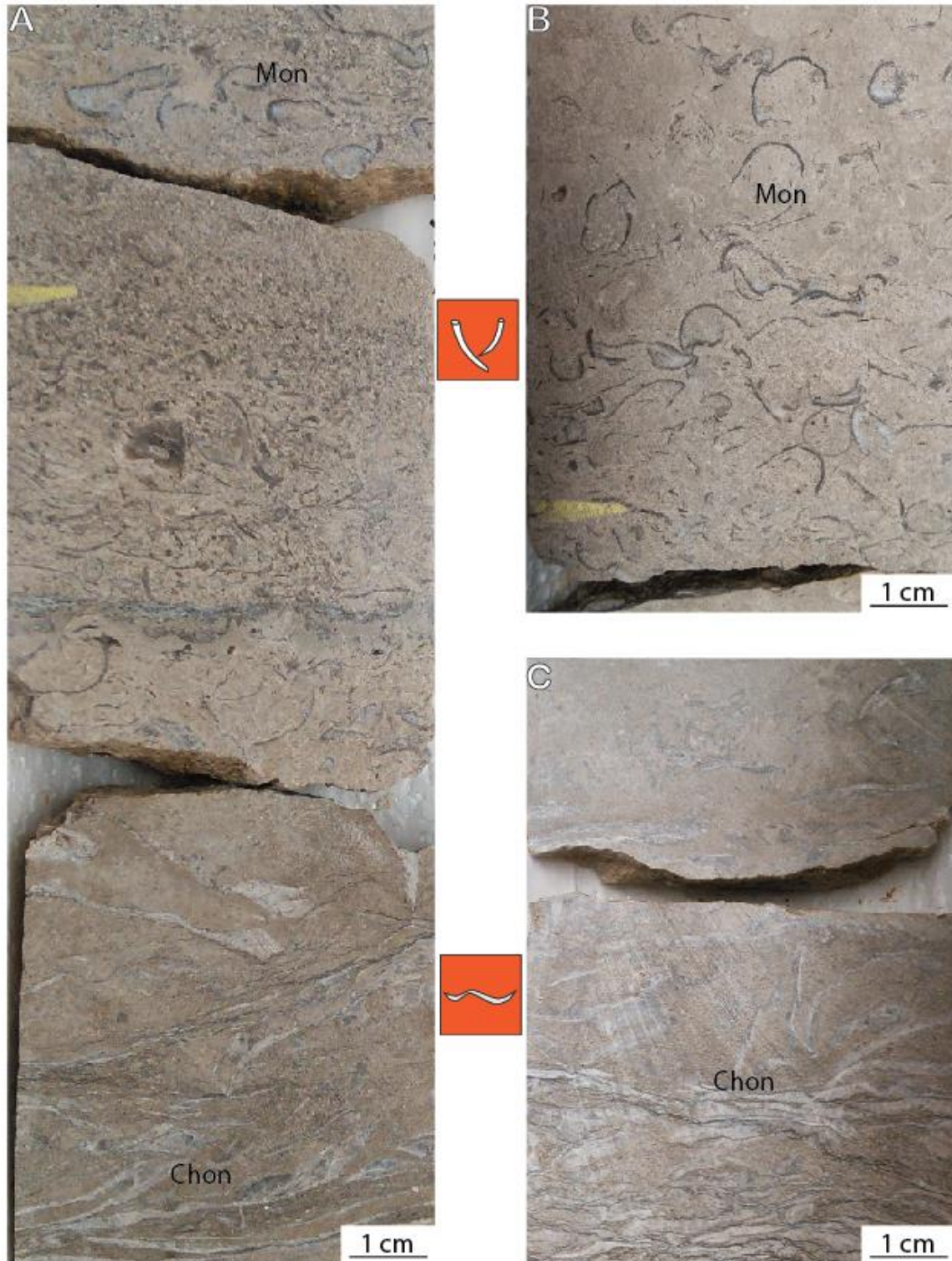


Figure 19: Monopleurid/Chondrodont floatstone. (A) Core slab showing an erosional surface in the middle of a monopleurid-chondrodont floatstone from Well 15-3 depth=11490 ft. (B) and (C) Core slabs showing monopleurid floatstone and chondrodont floatstone from Well 15-3 respectively.

MOLLUSCAN GRAINSTONE SHOREFACE/SHOAL

The molluscan grainstone of this facies assemblage is a superb reservoir facies (Kerans and Loucks, 2002). Abundant interparticle pore space with little or no carbonate mud lead to the favorable porosity-permeability relationships (Lucia, 1995) that are subject to and enhanced by meteoric dissolution. In South Florida Basin, molluscan grainstone likely represents a high-energy depositional setting such as a back-reef debris apron, tidal shoal-complex and carbonate beach in the South Florida Basin.

Facies Orb. G: *Orbitolina*-skeletal grainstone

Orbitolina grainstone comprises bivalve fragments, peloids, gastropods, and *Orbitolina* foraminifers. In thin section, heavily abraded bivalve fragments are commonly bored and subject to intensive dissolution with little carbonate mud. *Orbitolina* of this facies exhibit a higher aspect ratio (conical) at Sunoco Felda field than those at West Felda field. The tall, conical morphology of *Orbitolina*, in general, is commonly indicative of clear shallow water conditions (Immenhauser and Scott, 2002). In West Felda S4, the disk-like *Orbitolina* probably thrives in a relatively deeper water environment, periodically reworked into patch-reef debris aprons, and therefore interbedded with rudist rudstone, miliolids-peloid grainstone and ooid-skeletal grainstone. In Sunoco Felda, this facies overlies mollusc wackestone and represent a very shallow-water, small-scale tidal debris mound, which subsequently exposed to subaerial dissolution. During Lower Cretaceous time, *Orbitolina*-rich grainstone are interpreted as tidal-channel fill in the Mural Limestone at Grassy Hill, Arizona (Aisner & Kerans, 2010) (Aisner and Kerans, 2010) and in the Shuaiba Formation in the Middle East (Hamdan and Alsharhan, 1991).

Facies Mil. G: Peloid-miliolid-grainstone

Allochems are generally comprised of 80% miliolids, 10% peloids and 10% either chondrodonts or nondescript mollusk fragments. Gastropods and echinoids are rare. The low percentage of carbonate mud and well-sorted grain suggest a high-energy condition with constant winnowing/reworking. The massive unit of this grainstone in S-4 at well 35-4 (leeward sample) typifies this facies as upper-beach deposits and may occasionally be associated with washover deposits; and it may presumably be an excellent restricted-inner-

shelf shoreline indicator based on high abundance of miliolids, low diversity of fauna, and rare association with subtidal, intertidal sedimentary structure.

In S-4 at West Felda field, this facies features moderately higher percentage of bivalve fragments and rare presence of *Orbitolina* and commonly interbedded with rudist rudstone, *Orbitolina*-skeletal grainstone and miliolid-peloid packstone. Thus, it represents the beach deposits created by emergent rudist mounds. At Sunoco Felda field, this facies is vertically stacked with miliolid, peloid and gastropod dominated packstone-wackestone rock types; and further supports restricted, shallow-water tidal debris mounds.

Facies Ooi. G: Ooid-mollusk grainstone

This laminated grainstone shoal facies is composed of peloids, foraminifers, gastropods, micritized grains, coated grains, and bivalve fragments. Peloids vary in shape and size. *Orbitolina* is locally abundant. Micrite grains commonly enclose small fossils fragments. The ooid shoal facies commonly form as a physical barrier to current flow and therefore allow restricted lagoonal facies to accumulate shoreward (Scott R. , 1979). Thus, the ooid-mollusc grainstone in S-5 at well 31-2 overlies the rudist rudstone and may grade laterally into the massive miliolid-skeletal wackestone unit in S-5 at West Felda and Sunoco Felda fields; the ooid grainstone units at West Felda field may facilitate the accumulation of hypersaline lagoonal facies in S-5 at Sunoco Felda field.

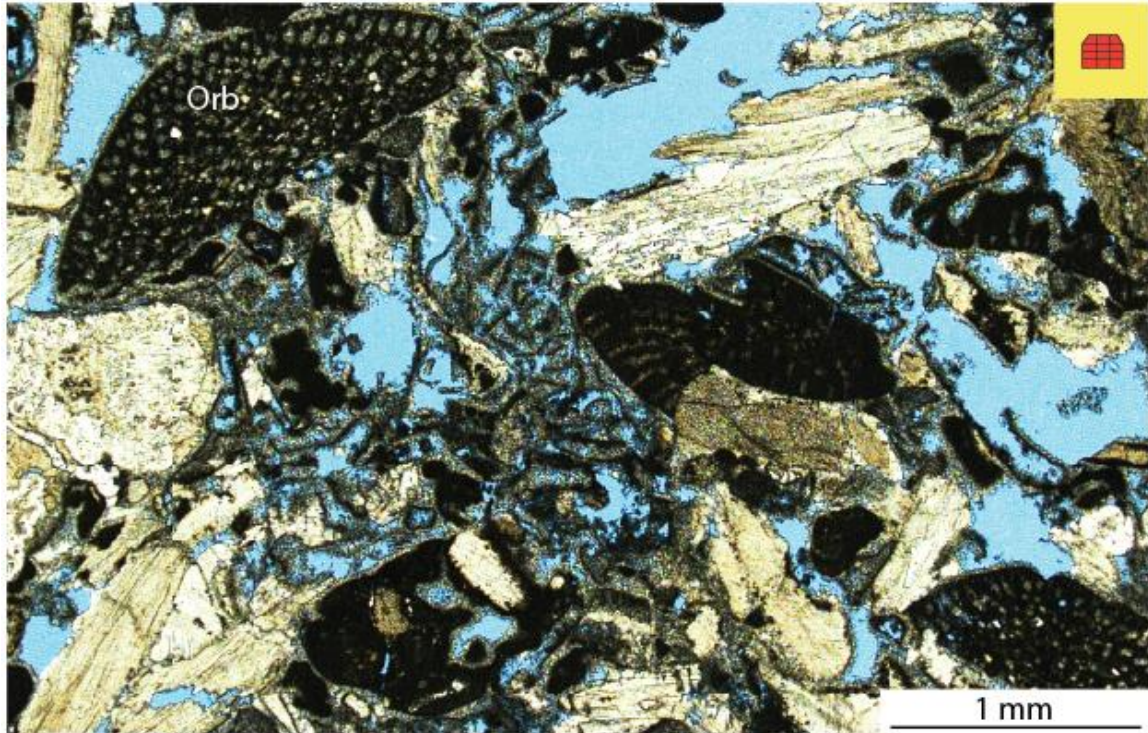


Figure 20: *Orbitolina*-skeletal grainstone, Well 28-3 depth=11526 ft.

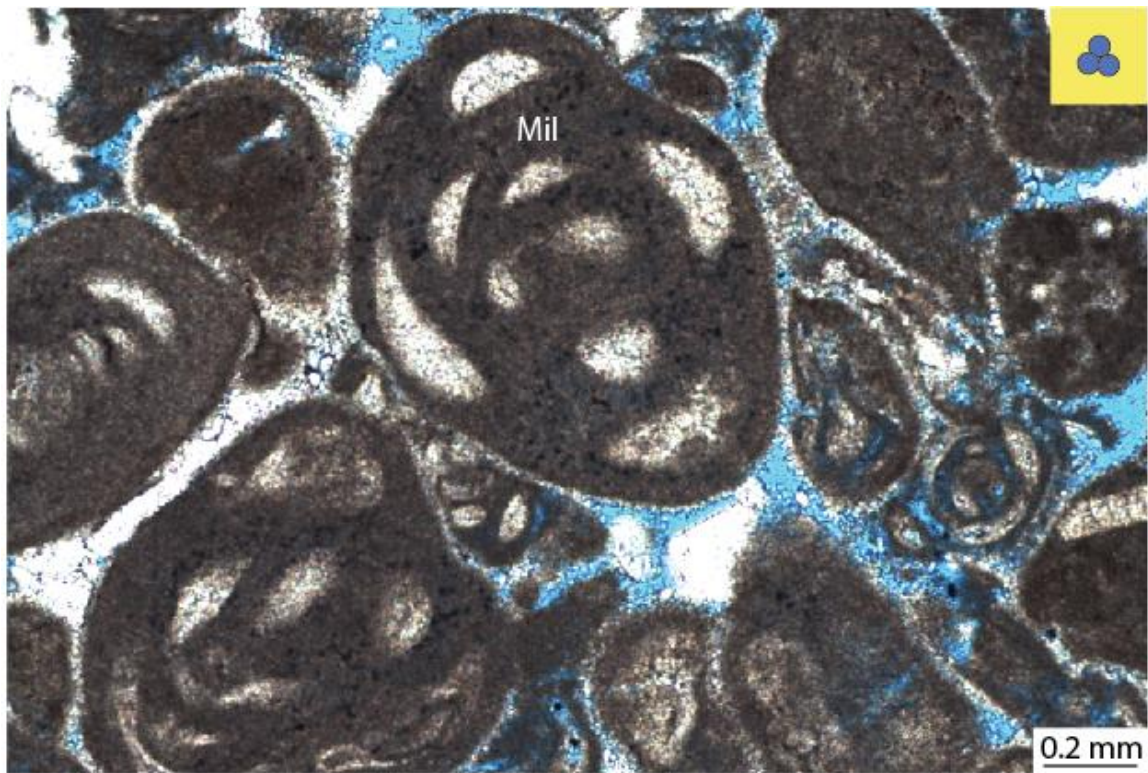


Figure 21: Miliolid-peloid grainstone, Well 35-4 depth=11377 ft. Miliolid (Mil).

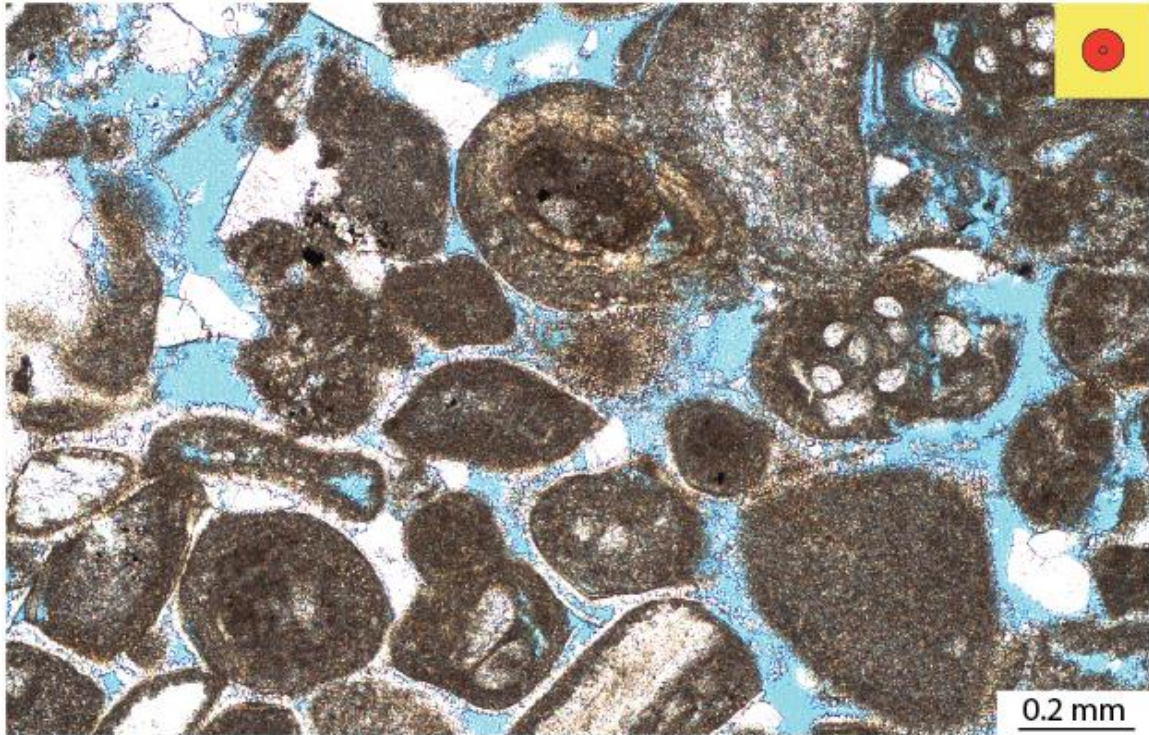


Figure 22: Ooid-mollusk grainstone, Well 29-3 depth=11457 ft.

Depositional Model

In East Texas, the deposition of the Ferry Lake Anhydrite occurred in a broad shelf lagoon, which was barred in the seaward direction by shelf-margin rudist bank buildups (Loucks and Longman, 1982). In South Florida, the Punta Gorda and Lake Trafford Formations present similar textures, lithology, sedimentary structures, fauna, and lamination types to the Ferry Lake Anhydrite. Therefore, the deposition of pre- and post-Sunniland anhydrites likely occurred in a mid-shelf environment behind the regionally extensive shelf-margin reefs. Previous studies (Rainwater, 1971; Feitz, 1976; Richards, 1988) indicates the failure and/or drowning of these shelf-margin reefs results in the deposition of Sunniland near-shore bioherms, biostromes, and grain shoals. Meanwhile, the stacked intertidal cycles and patch-reef growth patterns are similar to the observations from contemporary patch-reef outcrops in Texas and Arizona, all of which depict a distally steepened ramp profile. Thus, the Sunniland depositional profile during active growth of patch reefs can be interpreted as a distally steepened ramp. Figure 23 demonstrates the depositional model of the South Florida Basin during active reef-growth stage.

For this study, the ramp is divided into three areas, outer ramp, middle ramp and inner ramp. The lithologies of the outer ramp are primarily argillaceous lime wackestones and terrigenous mudstones in Texas (Hull, 2011) and Arizona (Aisner, 2011). Likewise, the argillaceous mudstone here is indicative of an outer ramp, deeper open-marine environment, where sediment was not subject to constant wave agitation, but may still have been subject to storm events. Landward of the argillaceous mudstone belt, *Orbitolina*-skeletal wackestone-packstone typifies the middle-ramp features including open subtidal shoal, mobile grain flats, and storm-lag deposits, which may serve as caprinid patch-reef nucleation points. Where the deep, open-marine facies interfingers with the open-marine subtidal facies, argillaceous lime mudstones and mollusk wackestones mark the transgressive portion of each depositional cycle. Whereas the *Orbitolina* mollusc lime packstones dominates the regressive portions and downdip grade into argillaceous lime wackestones. Rudist bafflestone best indicates the active growth of the caprinid rudist buildups in a middle-ramp, high-energy shoaling setting. Once the patch reef grew into such condition, it was episodically affected by waves and storms and surrounded by

skeletal debris aprons typified by rudist rudstones (Loucks, 1985). Leeward of the reef trend, the dolomitic, evaporitic, bioturbated mudstone-wackestone suggest a restricted hypersaline lagoon, where chondrodont mud mounds also occurred. The skeletal debris aprons of these bioherms provided much of the skeletal material incorporated into the beach complex (Kerans and Loucks, 2002). In Texas, the updip inner ramp facies are dominated by beach complexes (Kerans and Loucks, 2002). The peloid-miliolid packstone-grainstone here is associated with the shoreline setting adjacent to the sabkha-tidal flat area, which is best represented by algal-laminated mudstone and silty wispy-laminated mudstone-wackestone interbedded with anhydrite.

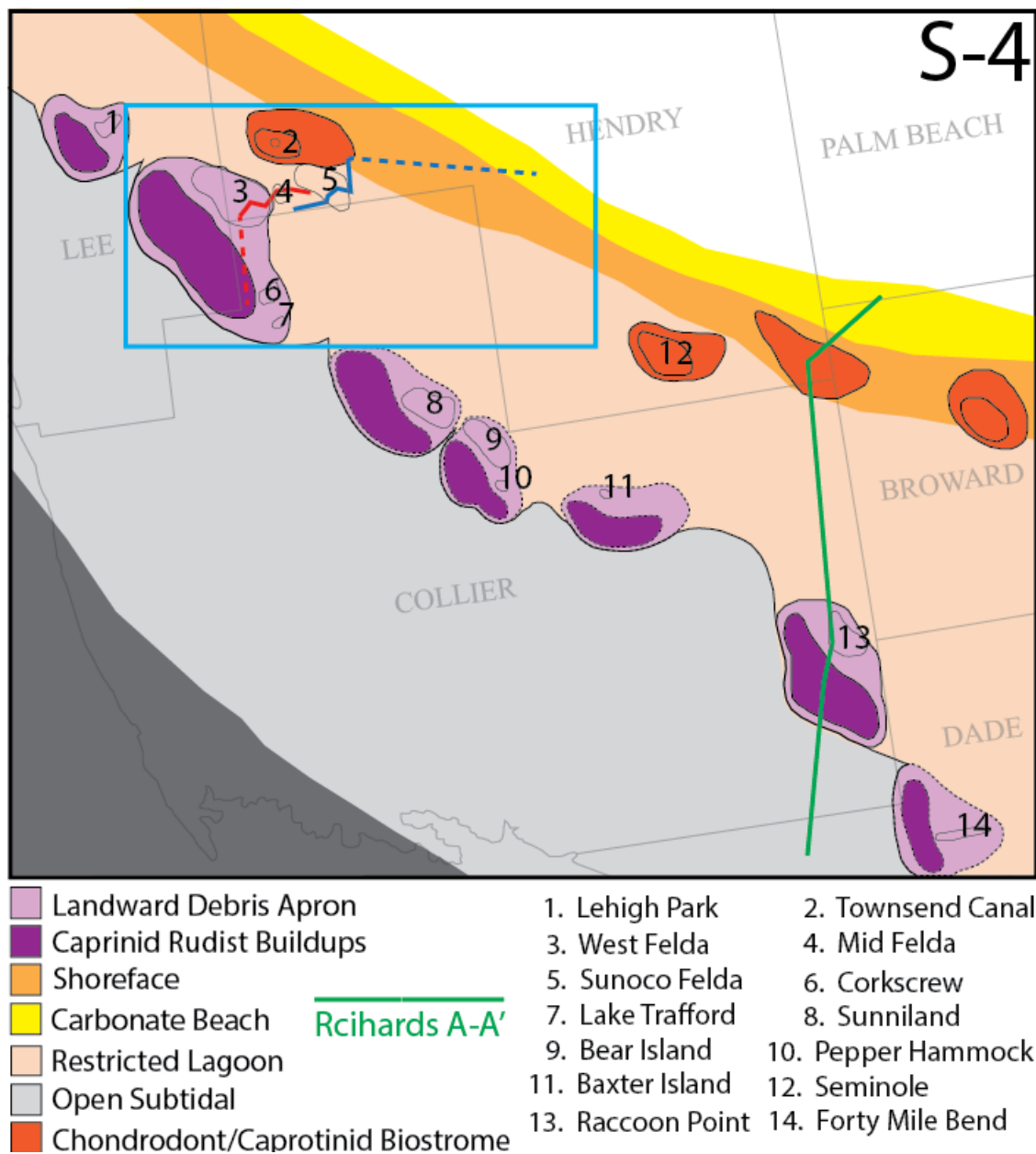


Figure 23: Facies and interpreted depositional environments of the Sunniland ramp interior in the South Florida Basin during the active growth stage of the caprinid reefs.

Ocean Anoxic Event 1B

The Cretaceous is a period of high eustatic sea level punctuated with a series of global oceanic anoxic events (OAEs). The primary driver of Cretaceous OAE 1B (Figure 2) is an increase in the rate of seafloor spreading and the emplacement of large igneous provinces (LIPs) in the South Pacific (Larson, 1991; Coffin and Eldholm, 1994; Bralower, 1999; Leckie, 2002; Phelps, 2011). It results in sea-level rise (Miller, 2005) and active volcanism (Jones and Jenkyns, 2001), which alter ocean chemistry, atmospheric CO₂ concentration, and add other nutrients such as Fe and Mg ions to the ocean (Jones and Jenkyns, 2001). Such a change in ocean chemistry and nutrient level results in a global biocalcification crisis (Erba, 1994; Bralower, 1999; Erba, 2010), thereby ultimately leading to anoxia, enhanced TOC preservation, and the demise of shelf-margin corals and rudists (Erba, 1994; Erbacher et al., 1996; Phelps, 2011).

In South Texas, this OAE 1B, like other OAEs, was critical in driving the transition from the flat-topped rimmed platform during the deposition of the Sligo Formation to the development of distally steepened ramp morphology during the deposition of the Bexar (Phelps, 2011) and Pearsall Formation (Hull, 2011). By synthesizing carbon isotope profiles, facies trends, and sequence stratigraphic interpretations from the Comanche Shelf, Phelps (2011) developed a four-phase model to demonstrate a full cycle of platform drowning and stabilization (Figure 24) in response to OAEs. First, during the initial equilibrium phase, the flat-topped rimmed platform assumes normal marine condition, shelf margin coral-rudist reefs and other phototrophic organisms. Second, the active volcanism of the crisis phase triggers a drastic shift in marine condition and results in decline of the coral-rudist assemblage at the shelf margin and oyster biostromes transgressed across the shelf with increasing accumulation of terrigenous shale. The subsequent anoxic phase condition causes the drowning of the carbonate platform into distally steepened ramp and is characterized by excursions in carbon isotope curves. Then, the recovery phase of the platform is characterized by diminished volcanogenic processes and re-establishment of the carbonate factory in bathymetrically shallow-water areas near the shoreline.

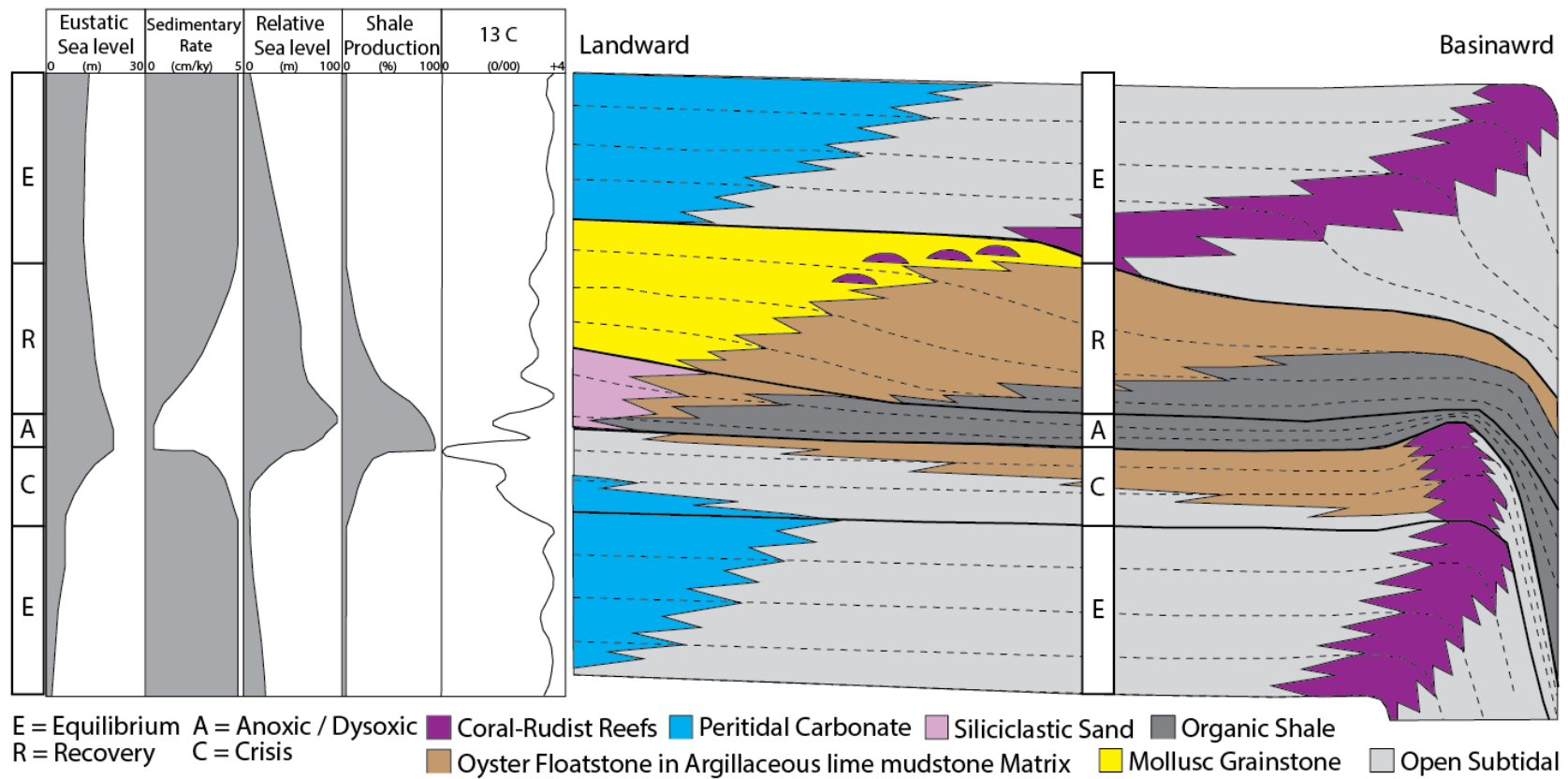


Figure 24: Phelps (2011) Schematic four-stage model shows the effect of OAEs on cycles (2011). Figures reproduced with permission by R. Phelps (2011). Graphs at left are a summary of multiple supersequences with estimated values for eustatic sea level, relative sea level, and shale proportion. The $\delta^{13}C$ curve is schematic.

Stratigraphy

SUMMARY OF APPROACH

The Sunniland shoreline to shelf edge sequence stratigraphic model (Figure 25) incorporates two lines of cross section (Figure 3). The blue line extends from the leeward-most position (Alico 35-4) across most of the Sunoco Felda field. The red line runs further to the west across Mid Felda and West Felda fields and reaches the most basinward data point, Alico 31-2. Wireline logs spread along the line of section are used to constrain the correlations. Cycles and sequences were tied to the raster and gamma ray logs based on the Atlas of Log Responses (Page and Miller, 2002) from Baker Hughes.

The basin-wide facies maps (Figure 26) is based on the sequence analysis of the shelf-interior facies succession in the FSU and Raccoon Point fields (Figure 7 and 8) and synthesis of the regional paleogeographic information from previous studies. In addition, Mitchell-Tapping (1985) petrographic study on Sunniland, Bear Island and Forty Mile Bend fields provides extra data control by presenting the characteristics of the major lithofacies associated with these fields.

Generally speaking, the inner- and middle-ramp stratigraphic architectures react more responsively and distinctively to the changes in marine condition and accommodation as compared to the outer ramp. Thus, the analysis of FSU data may have constructive implications in predicting the outer-ramp stratigraphic architectures. The following sections detail the internal characteristics of each of the five depositional cycles (S-1 to S-5), including the component lithostratigraphic units, facies distributions, high-frequency cycles, depositional environments, and platform-scale morphologies.

GENERAL STATEMENT

In South Florida, the stratigraphic position and the dominance of the high TOC, argillaceous mudstone in the lower section of the Sunniland Formations suggest that the onset and recovery of the OAE 1B and the associated transgression are likely the main drivers on the lithofacies variation in the Sunniland Formation. Thus, Phelps (2011) four-stage model may help unravel the evolution of this system from shoreline to shelf-margin (Figure 25). In reference to Phelps' model, first, the transgressive facies pattern atop the Punta Gorda Anhydrite might represent the crisis stage. Second, the anoxic stage was likely coincident with deposition of the high TOC, argillaceous mudstone (Hull, 2011; Phelps, 2011). Subsequently, during the early recovery stage, the carbonate factory dominated by chondrodontids and monopleurids re-established near the shoreline, and sediment accumulation rates slowly increased as dysoxia diminished. Then, the full recovery stage is marked by the active growth of caprinid patch reefs.

However, unlike its counterparts in Texas and Arizona, the South Florida Basin is unique for its continuous carbonate-evaporite deposition. This is mainly due to two factors. First, the South Florida basin is more proximal to the equator. Thus, the surface water temperature is relatively high, leading to more rapid evaporation and elevated salinity. Second, unlike in Texas, there was little to no siliciclastic input of fresh water to balance elevated salinity, leaving the entire shelf in a long-lasting hypersaline condition. Such condition may lead to a time of immense stress and thereby results in the disappearance of the near-shore habitats for rudists. Meanwhile, during the full recovery stage, rudist larvae may have been carried along with planktons in surface currents (Johnson, 2002) and reestablish the caprinid communities around the Cretaceous Florida Escarpment. The reestablished communities may eventually result in a change to low angle, rimmed-shelf depositional profile, barring the South Florida Basin from the open ocean and facilitating the deposition of the overlying Lake Trafford Anhydrites, which likely marks the equilibrium stage.

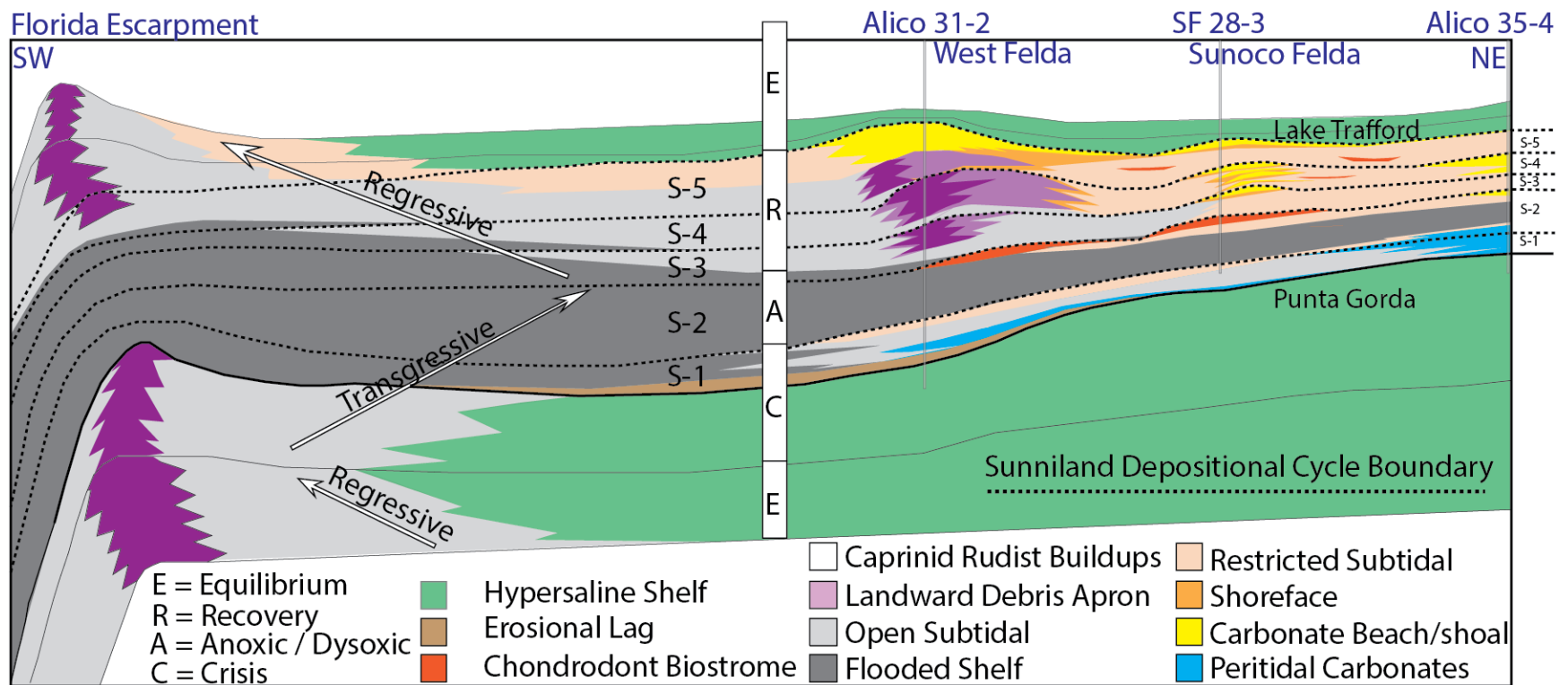


Figure 25: Response of the platform to OAE 1B, showing schematic profiles and simplified lithofacies distributions on the South Florida Shelf prior to, during, and following OAE 1B. Characteristics of the equilibrium, crisis, anoxic/dysoxic, and recovery phases are discussed in the text.

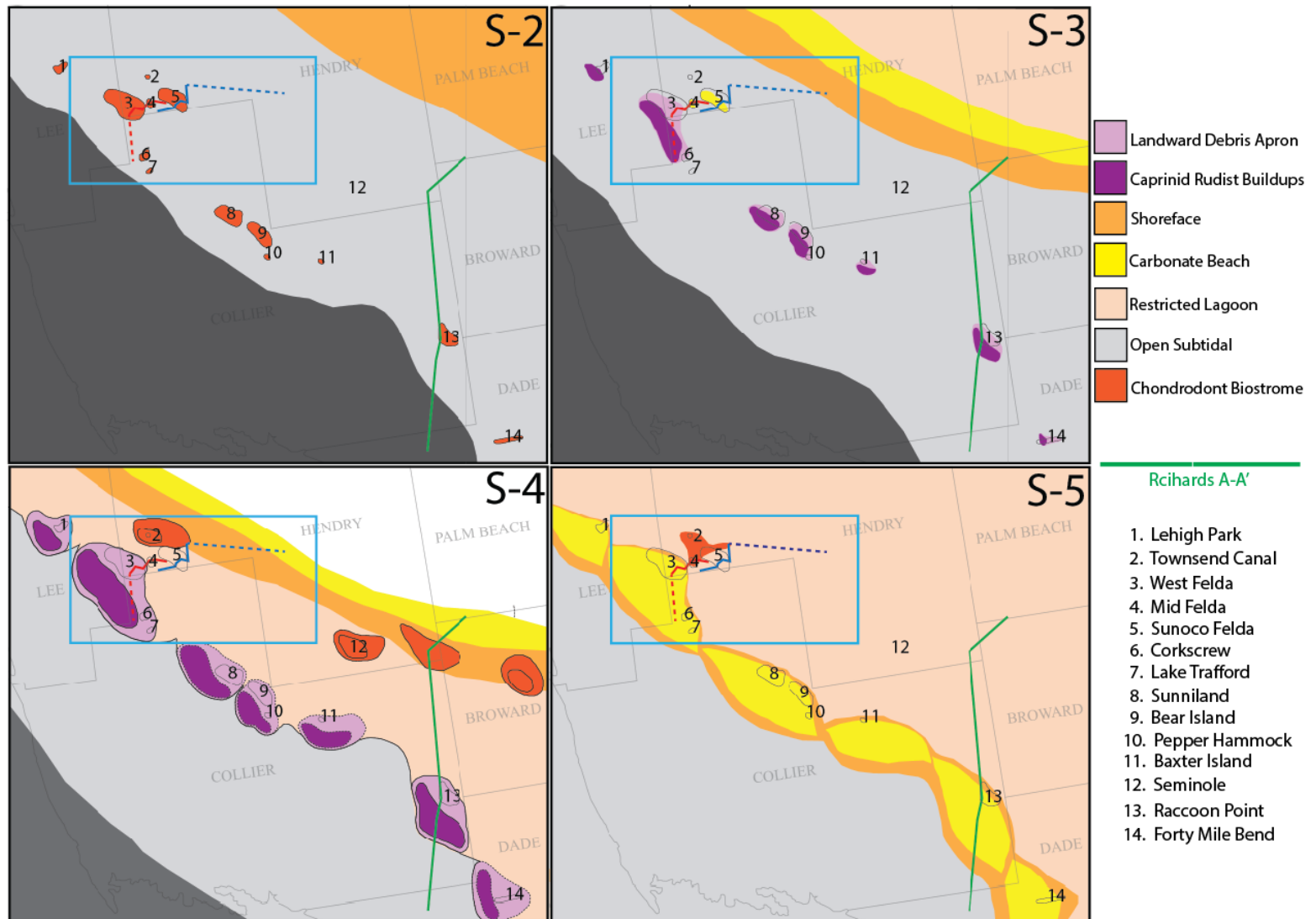


Figure 26: Sunniland lithofacies maps in the South Florida Basin of S-2 to S-5 depositional cycle, respectively.

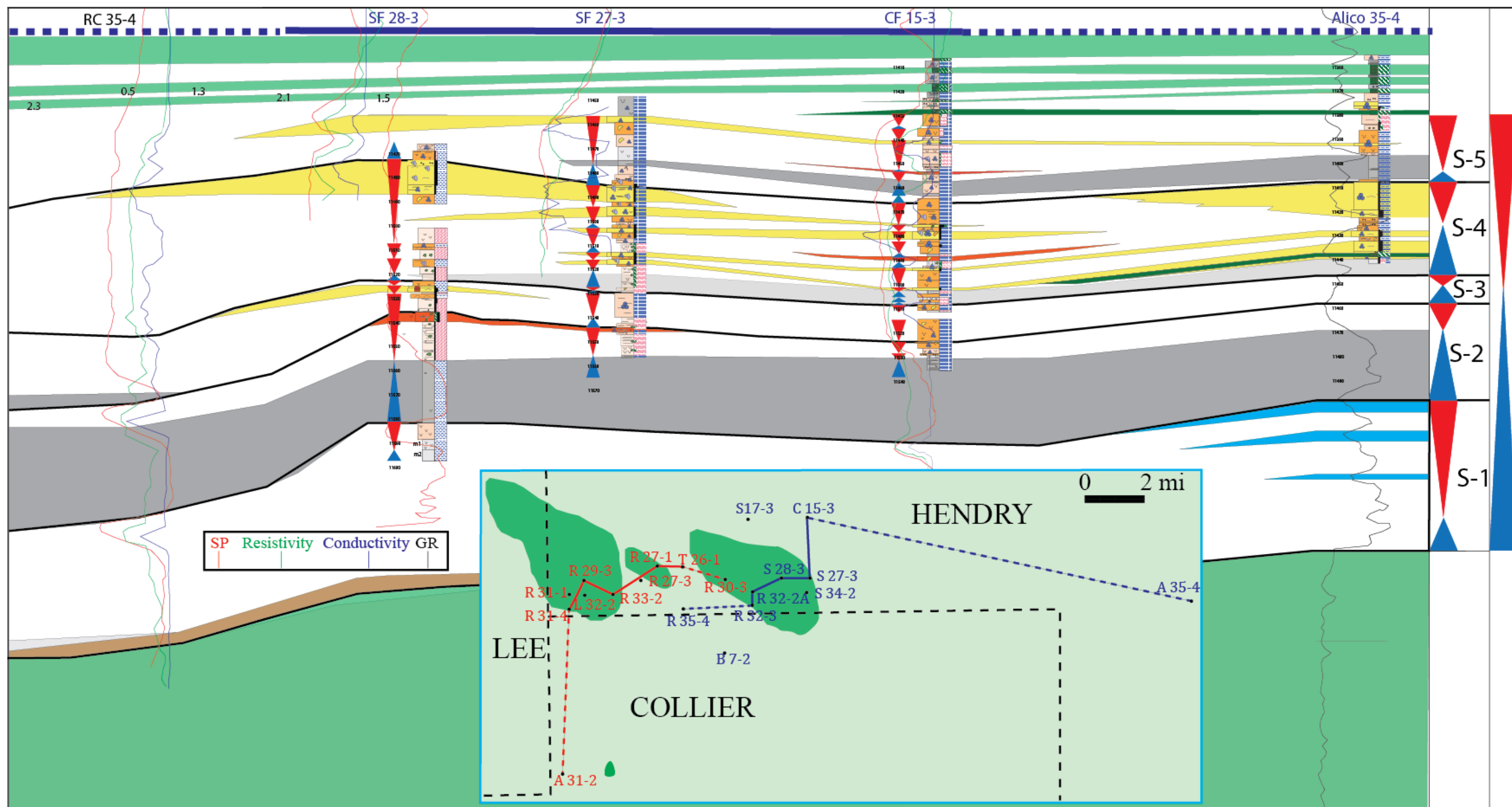


Figure 27: The blue line extends from the leeward-most position (Alico 35-4) across most of the Sunoco Felda field.

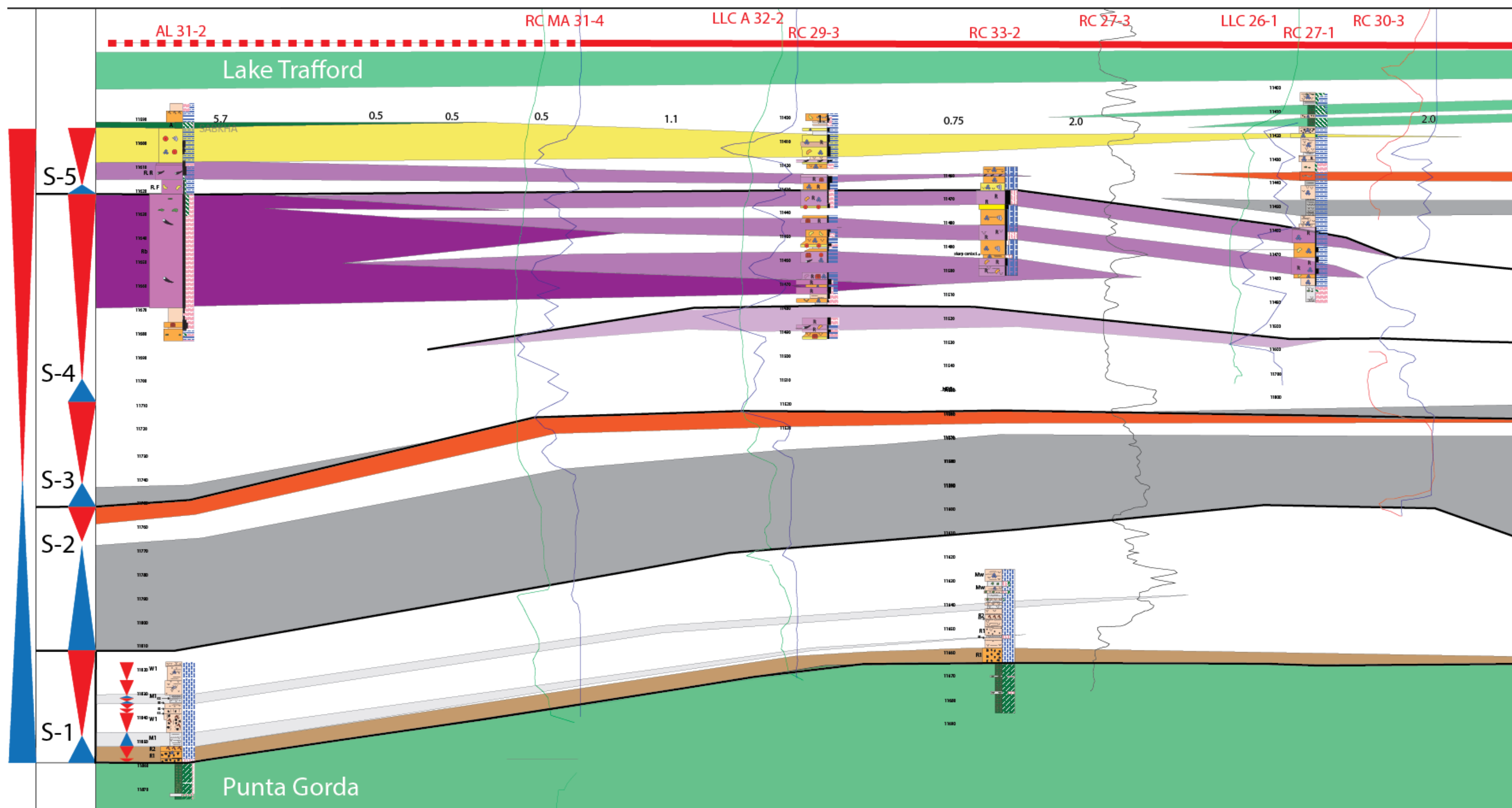


Figure 28: The red line runs further to the west across Mid Felda and West Felda fields and reaches the most basinward data point, Alico 31-2.

SUNNILAND DEPOSITIONAL CYCLE-1 (CRISIS PHASE)

In cores from Alico 31-2 and RC 33-2 (S-1, Figure 28), the erosional lag immediately overlies the Punta Gorda anhydrites with a sharp contact, which marks the lower boundary of the Sunniland Formation and may further extend to the Sunoco Felda field area. The diameter of some intraclasts within this erosional lag is up to 4 cm. It may suggest a product of a significant storm event, transgressing sediments from ravinement surface. Further transgression results in a subtidal unit of skeletal mudstone. The increase fauna diversity in this unit indicates a shift to a relatively open-marine but low-energy subtidal shelf environment. The subsequent exposure surface complex is a set of 3-4 supratidal-subtidal high-frequency cycles. The high-frequency cycle top is marked by root burrows and soil-like diagenetic textures (Loucks, 1985) as an indication of exposure surface with vegetation. These high-frequency cycles cannot be confidently correlative between Alico 31-2 and RC 33-2 but they are collectively correlated as one cycle set along the dip-orientation, and thereby indicate a period of relatively high eustatic amplitude and frequency. Then, the next subtidal unit indicates a further deepening of the system. Yet, the increase of nodular anhydrite and decrease of fauna diversity at top of this unit at RC 33-2 may suggest an increase of salinity due to the lowering of sea level. Such eustatic change may also be corroborated by a prograding trend based on the gamma ray signal at RC 35-4 (S-1, Figure 27).

In East Texas, the deposition of the Ferry Lake Anhydrite occurred in a broad shelf lagoon, which was barred in the seaward direction by shelf-margin rudist bank buildups (Loucks and Longman, 1982). In South Florida, the Punta Gorda Formation is comparable with the Ferry Lake Anhydrite in terms of lithology and sedimentary structures. Thus, like in East Texas, the underlying Punta Gorda Formation likely occurred in a mid-shelf environment behind the regionally extensive shelf margin reefs (Figure 25). In south Texas, peritidal carbonates commonly prograded across much of the low-angle shelf-interior, leaving a significant portion of the shelf profile within an intertidal setting (Phelps, 2011). Therefore, in South Florida, the stratigraphic position and the dominance of peritidal carbonates may suggest much of the deposition in S-1 occurred on a low-angle shelf-interior environment barred from the open ocean by the dwindling shelf margin reefs, indicating a crisis phase (S-1, Figure 25).

SUNNILAND DEPOSITIONAL CYCLE-2 (ANOXIC/DYSOXIC PHASE)

The S-2 depositional cycle comprises a high-TOC argillaceous mudstone unit and a chondrodont floatstone unit. The argillaceous mudstone unit dominates the S-2 sequence at Sunoco Felda (S-2, Figure 27). Based on log responses, it thickens basinward to West Felda and Alico 31-2 fields. The USGS carbonate-source-rock study (Palacas, 1984) concludes this high TOC unit as the major source of the upper Sunniland oil based on detailed crude-oil-source correlations including gas-chromatographic-mass-spectrometric analysis of steranes, and of tricyclic and pentacyclic terpanes and provide the isopach of this high TOC unit. In South Texas, the extensive deposition of argillaceous lime mudstone in the upper Bexar supersequence and lowermost Glen Rose indicates a significant shift to a deep open-marine depositional environment on a flooded shelf (Phelps, 2011). Meanwhile, in the more distal Pearsall Formation, outer ramp OAE facies are siliciclastic-dominated, TOC-rich, and little-bioturbated (Hull, 2011). Thus, the deposition of the TOC-rich, argillaceous mudstone unit here are likely resulted from the OAE-1B and the associated transgression, which accentuates the rimmed shelf profile in S-1 into a distally steepened ramp profile (S-2, Figure 25).

In South Texas, recovery of the OAE-1B starts with the near-shore reestablishment of the carbonate factory dominated by chondrodontids and monopleurids (Hull, 2011; Phelps, 2011). The sediment accumulation rate slowly increased as dysoxia diminished. Thus, in South Florida, the upward transition from argillaceous mudstone to chondrodont floatstone in S-2 may reflect the sporadic resumption of carbonate sedimentation. On the facies map (S-2, Figure 26), the outer-ramp facies are the flooded shelf mudstones/wackestones; the middle-ramp facies are mud-dominated chondrodont floatstone and the inner-ramp may present shoreface grainstone facies.

SUNNILAND DEPOSITIONAL CYCLE-3 (RECOVERY PHASE)

The cores from RC 29-3 (S-3, Figure 28) include an *Orbitolina*-skeletal grainstone unit and an overlying rudist rudstone unit, indicating the possible existence of a rudist biostrome within the uncored interval at Alico 31-2. Based on log responses, a series of retrograding HFC of subtidal shelf wackestone-packstone may exist beneath this *Orbitolina* skeletal grainstone. Landward of the section, in cores from Sunoco Felda (S-3,

Figure 27), the mudstone/wackestone unit with anhydrite nodules overlies the chondrodont floatstone unit in S-2 and marks the base of the S-3. At SF 28-3, the mudstone unit is capped by an *Orbitolina*-skeletal grainstone unit. This unit has the first and only appearance of *Orbitolina* among all Sunoco Felda cores. Thus, the grainstone unit here may suggest a channel bar formed during flooding events, transgressing *Orbitolina* from a deeper normal marine location. In South Texas, Phelps (2011) places the maximum flooding of the lower Glen Rose Formation above retrograding HFC Sets of subtidal shelf wackestone-packstone within the retrograding *Orbitolina* packstone, leaving the subsequent widespread caprinid bioherms deposited during early highstand. Thus, in South Florida, the first and only appearance of *Orbitolina* in Sunoco Felda, the presence of caprinid patch reef complex over the *Orbitolina* wackestone facies in Alico 31-2 and the West Felda field support that the maximum flooding of the Sunniland depositional sequence lies within S-3.

SUNNILAND DEPOSITIONAL CYCLE-4 (RECOVERY PHASE)

In cores from Alico 31-2 (S-4, Figure 28), the 10-ft *Orbitolina*-skeletal wackestone unit is characterized by the abundance of carbonate mud, disk-like morphology of *Orbitolina*, and the diverse marine fauna, all of which suggest a well-oxygenated and well-lit normal marine condition. Such condition is commonly associated with stable substrates for patch-reef nucleation (Scholle, 1983) and therefore created a hospitable environment for the solitary rudist to thrive and aggregate into middle-ramp rudist bioherms evidenced by the overlying 50-ft caprinid bafflestone complex. Once the bioherms grew into a high-energy shoaling condition, they are episodically affected by waves and storms and surrounded by skeletal debris aprons, forming a trend of middle-ramp high-energy shoal complexes (Loucks, 1985). This trend may dampen the wave energy and results in a restricted inner-ramp environment. In addition, anhydrite nodules within the top of the caprinid bafflestone complex may indicate elevated ocean salinity. The overlying exposure surface indicates a period of significant sea-level drop, marking the top boundary of S-4.

The correlation of each high-frequency cycle in cores from West Felda (S-4, Figure 28) represents excellent planar wedge-set stratification, alternating rudist rudstones and miliolid-skeletal packstones. The occasional appearances of nearly whole caprinids are

likely results of major storm events. Meanwhile, local topography may provide the relatively lower energy shelter for the *toucasids* (Loucks, 1985) found within miliolid-skeletal packstones.

Relative sea-level change is the key controlling factor over the cyclicity in the restricted shelf-interior setting. Thus, landward of the section at Sunoco Felda (S-4, Figure 27), the HFC here is characterized by the transition from miliolids wackestone to grainstone. Over the course of successive HFCs, the abundance of gastropods increases, indicating increasingly stressed conditions. The correlation between these HFCs is based on the shoreline migration trend, evidenced by the facies succession of the beach deposits in Alico 35-4.

In South Texas, the absence of shelf-margin reef barriers allowed circulation of normal marine water into the platform interior and promoted growth of rudist patch reefs (Phelps, 2011). In South Florida, the lateral and vertical facies successions of the caprinid patch reefs here are analogous to the observations at the lower Glen Rose caprinid-patch-reef outcrop in Red Bluff, Texas. Thus, S-4 may have a distally steepened ramp profile, similar to the lower Glen Rose formation. The patch reefs here are likely representative of the normal marine middle-ramp environment, whereas the basinward tidal shoal complexes of peritidal grainstones and mudstones have the characteristics of the inner-ramp deposits. Yet, towards the top boundary of this depositional cycle, the presence of anhydrite nodules within the top of the caprinid baffestone complex at Alico 31-2 and the increasingly abundant algal-feeding gastropods within the tidal shoal complex at Sunoco Felda indicate an increasingly restricted marine condition.

SUNNILAND DEPOSITIONAL CYCLE-5 (RECOVERY TO EQUILIBRIUM PHASE)

The rudist floatstone unit at Alico 31-2 (S-5, Figure 28) exhibits a sharp contact with the underlying rudist baffestone complex, marking the initiation of S-5. This floatstone unit may indicate an open-marine, low-energy setting during transgression and may correlate to the argillaceous mudstone unit and the overlying chondrodont floatstone unit at Mid Felda and Sunoco Felda fields (S-5, Figure 27). Above the floatstone unit, the overlying rudstone unit is suggestive of a relatively smaller rudist patch reef developed windward of Alico 31-2 and indicates a high-energy shoaling condition based on the

abundance of dissolved bivalve fragments, presence of *Lithocodium/Bacinella* and the absence of carbonate mud. Such shoaling condition continues and results in an ooid shoal developed above. Ooid shoals commonly act as physical barriers to current flow and therefore allow restricted lagoonal facies to accumulate shoreward (Scott R. , 1979). Thus, the development of this ooid-shoal unit results in the deposition of the dolomitized, anhydrite nodules miliolid-skeletal wackestone unit at West Felda and Sunoco Felda fields, which is suggestive of a hypersaline lagoonal environment.

Landward of this sequence, in cores from Sunoco Felda field (S-5, Figure 27), the reoccurrence of the argillaceous lime mudstone may indicate a brief transgression marine and correlates with the rudist floatstone unit at Alico 31-2. The overlying chondrodont biostromes at RC 27-1 and CF 15-3 may indicate sporadic resumption of carbonate sedimentation after a brief marine transgression. The correlation between the tidal flat-capped, HFC here shows a progradational trend. Over the course of succession, a series of intercalated sabkha-supratidal-intertidal sediments marks the transitional contact with the overlying Lake Trafford Formation at RC 27-1, CF 15-3, and Alico 35-4. This series of sediments and the appearance of sabkha units at Alico 31-2 indicate a shift to a more restricted marine condition. Such conditions lead to a time of immense stress and the disappearance of the near-shore habitats for rudists. Nevertheless, rudist larvae, like those of many modern bivalves, may have been carried along with planktons in surface currents (Johnson, 2002) and re-establish the caprinid communities around the Cretaceous Florida Escarpment. The re-established caprinid communities may eventually result in a change to the rimmed-shelf depositional profile, similar to S-1, barring the South Florida Basin from the open ocean and facilitating the deposition of the overlying Lake Trafford Anhydrites.

Pore Network

The lowered sea level in S4 enhanced the reservoir quality in the high-energy settings including back-reef debris aprons, tidal shoal-complex and carbonate beach. In these settings, subaerial exposure and freshwater phreatic diagenesis preserved high, primary interparticle porosity with the favorable porosity-permeability relationships, producing the Sunniland reservoir facies (Figure 18, 20, 21, 22). In addition, some dolomitized rudist bafflestones (Figure 29) exhibit sucrosic texture and excellent intercrystal porosity, which also serve as excellent reservoir rocks.

The sabkha-tidal flat facies in S5 forms the permeability barrier, overlying the reservoir facies. The absence of an open-flow system would result in less calcite cementation, preservation of much of the primary interparticle porosity and maintain the reservoir quality (Loucks, 1977). Thus, the permeability barrier in S-5 prevented the destruction of most primary interparticle and moldic porosity in the reservoir facies by inhibiting further cementation by calcite-rich pore fluids and non-calcitic pore-reducing minerals.

Above the high TOC, argillaceous chalk in S2, the medium-fine crystal dolomites within or surrounding S-3 (Figure 27) were originally deposited as lime mud and recrystallized into dolomite, exhibiting fair intercrystal porosity. The average crystal size here is generally larger than the dolomitized sabkha-tidal flat facies in S-5. Thus, the dolomite here (Figure 30) may not adversely affect and likely facilitate the migration of hydrocarbon self-sourced from the high TOC, argillaceous chalk in S2 to the reservoir facies in S-4.

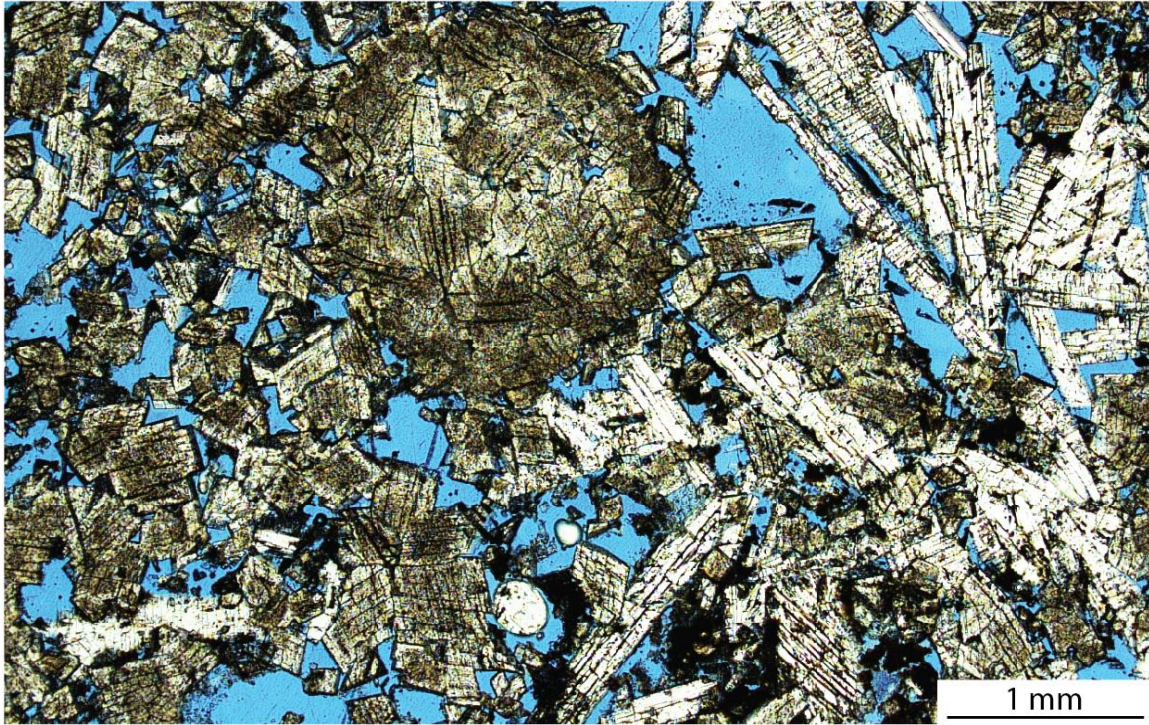


Figure 29: Dolomitized Rudist Bafflestone. Note some anhydrites crystal (right), Well 31-2 depth=11628 ft.

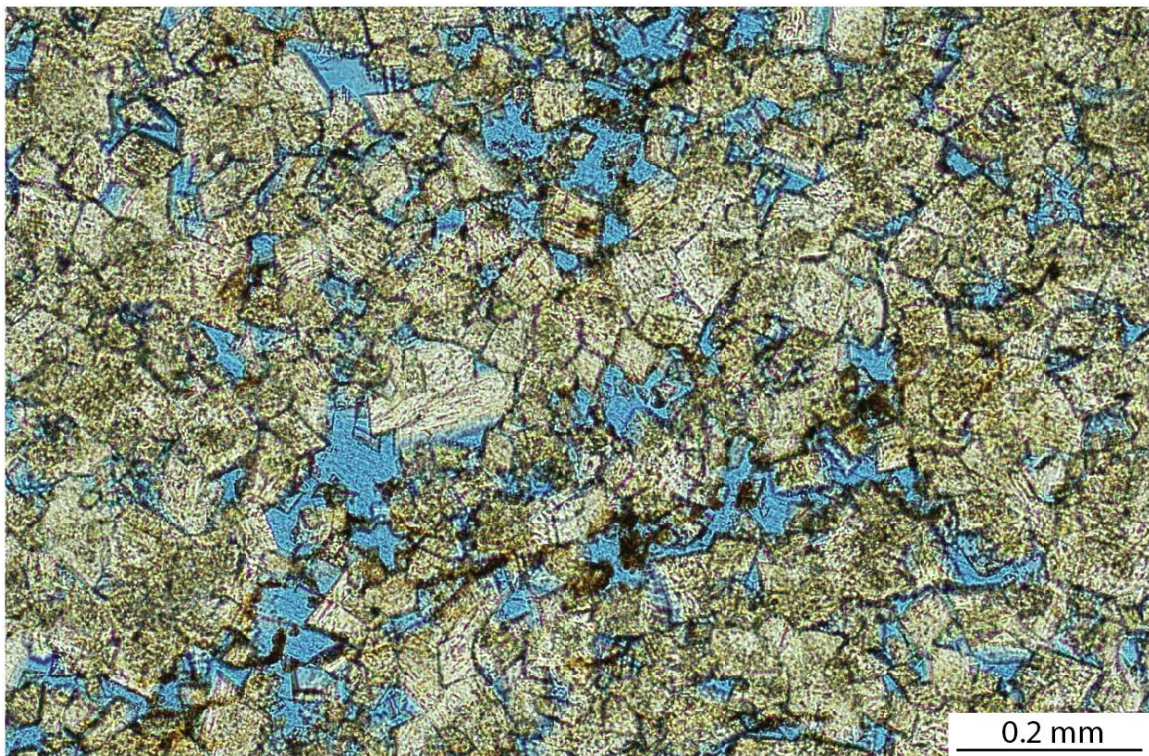


Figure 30: Dolomitized Skeletal Wackestone, Well 28-3 depth=11535 ft.

Conclusion

The Sunniland Formation was deposited during a major transgressive-regressive sequence. The Sunniland interval is divided into five third-fourth order, transgressive-regressive depositional cycles (S-1 to S-5) in South Florida using sequence analysis of shelf-interior facies succession. In these depositional cycles, facies proportion, faunal composition and stratal geometries of the shelf-interior are found to be the result of the changing accommodation trends and ocean chemistry. As in the Comanche Platform in South Texas, the detrimental effects of oceanic anoxic event 1B may fundamentally drive the evolution of platform morphology in the eastern Gulf of Mexico as:

- Rimmed shelf (Crisis phase: S1)
- Distally steepened ramp (Anoxic/dysoxic phase: S2, recovery phase: S3, S4)
- High-angle rimmed shelf (recovery to equilibrium phase: S5)

Within this hydrocarbon-producing trend, the lowered sea level at the end of S4 enhances the reservoir quality in the high-energy settings including back-reef debris aprons, tidal shoal-complex and carbonate beach by dissolution. The tight sabkha-tidal flat facies in S5 forms the reservoir seal, whereas the medium-fine crystal dolomites in S3 may not adversely affect and likely facilitate the migration of hydrocarbon self-sourced from the high TOC, argillaceous chalk in S2.

In Texas, OAEs have been detected by excursions in carbon isotope curves (Hull, 2011; Phelps, 2011) and are times of major extinction and radiation of (Aconcha, 2008) nanofossils (Erba 1994; Erbacher et al., 1996). Thus, future work should focus on the Cretaceous secular carbon isotope profile and biostratigraphy to corroborate my sequence model (Figure 25).

Appendix A

Sunniland Symbol Key

Lithology



Dolomite



Limestone

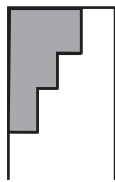


Anhydrite



Porosity

Relative Abundance



Abundant
Common
Present

Structure



Parallel



Wispy



Burrows



Roots



Burrows or Roots



Vertically Aligned
Mosaic Anhydrite



Bedded Nodular
Mosaic Anhydrite



Anhydrite Nodule



Anhydrite

Allochems



Clasts



Ooids



Skeletal fragment



Mud



Miliolids



Gastropod



Caprinids



Toucasids



Oyster



Monopleurid

Facies



Grainstone



Rudstone



Bafflestone



Packstone



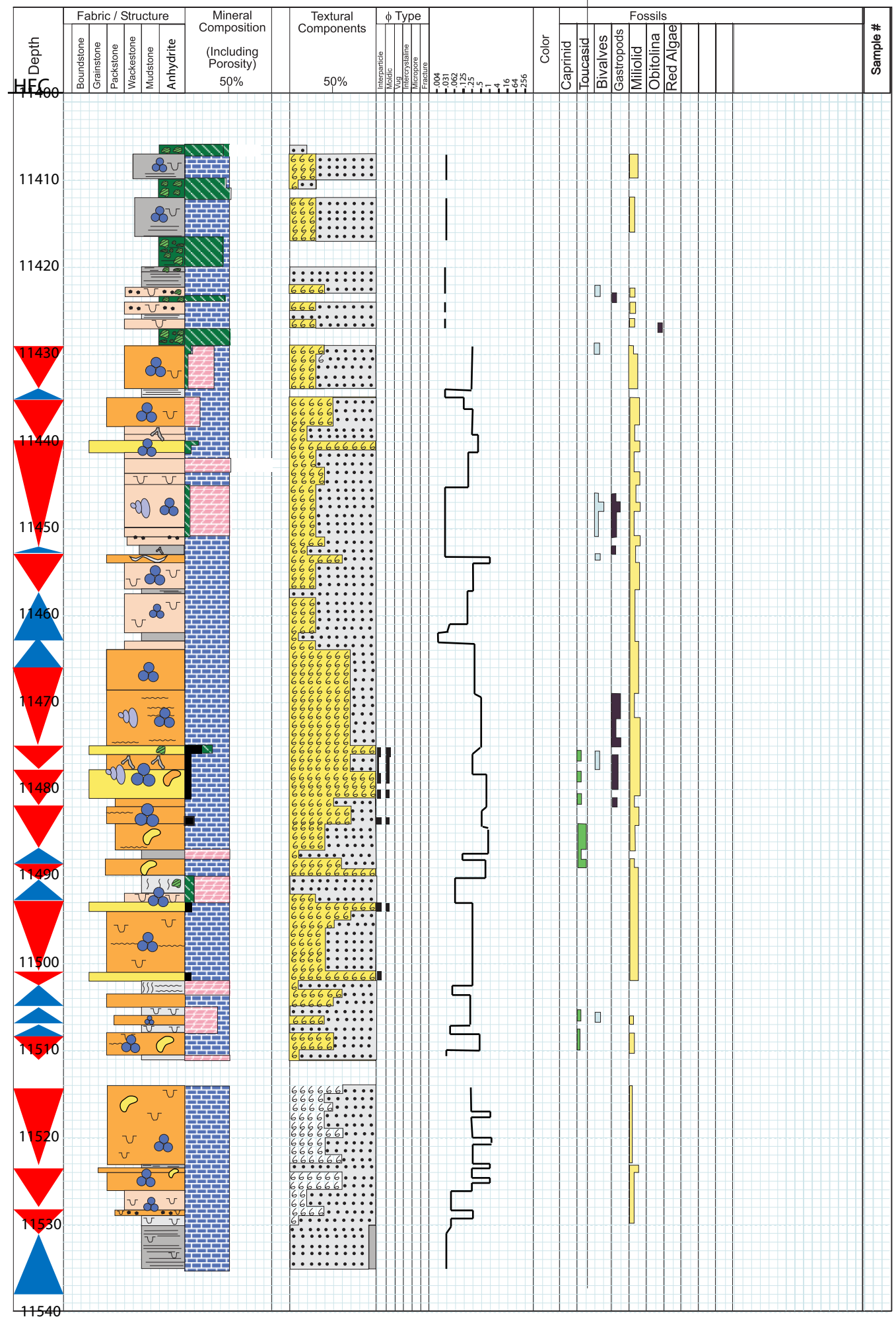
Wackestone



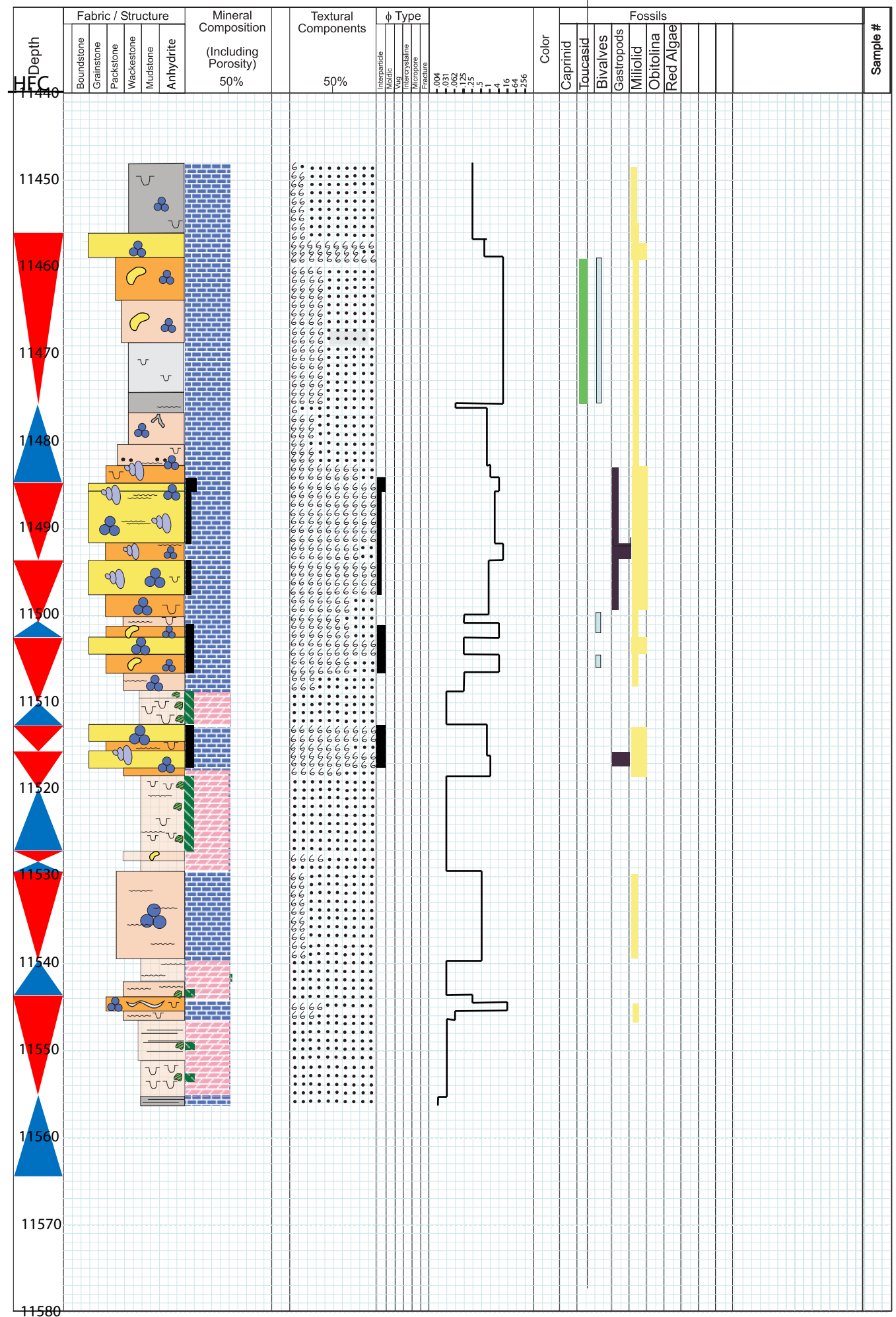
Mudstone



Floatstone



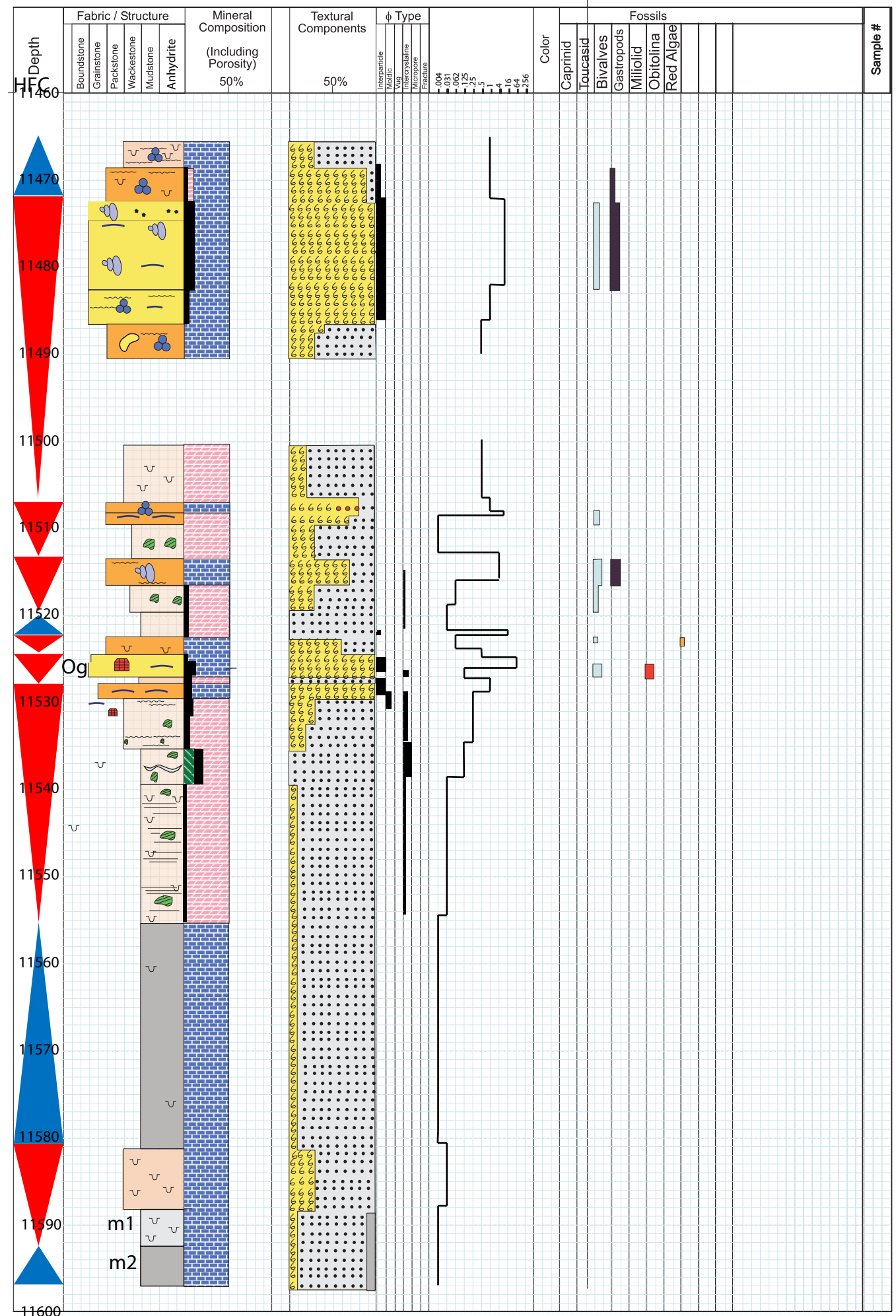
Depth	Fabric / Structure					Mineral Composition (Including Porosity) 50%	Textural Components 50%	φ Type						Color	Fossils										Sample #
	Boundstone	Grainstone	Packstone	Wackestone	Mudstone			Anhydrite	Interparticle	Moldic	Vug	Crystaline			Microzone	Fracture	Caprinid	Toucasid	Bivalves	Gastropods	Miliolid	Obitolina	Red Algae		
11390																									
11400																									
11410																									
11420																									
11430																									
11440																									
11450																									
11460																									
11470																									
11480																									
11490																									
11500																									
11600																									
11700																									
11800																									



Location: Collier, FL

Logged By: CXL

Date:



Depth	Fabric / Structure					Mineral Composition (Including Porosity) 50%	Textural Components 50%	ϕ Type						Color	Fossils										Sample #
	Boundstone	Grainstone	Packstone	Wackestone	Mudstone	Anhydrite		Interparticle	Moldic	Dolomitized	Microcrystalline	Microvoid	Fracture		Caprinid	Toucasid	Bivalves	Gastropods	Miliolid	Obitolina	Red Algae	Chondrodont	Monopleurid		
11390																									
11400																									
11410																									
11420																									
11430																									
11440																									
11450																									
11460																									
11470																									
11480																									
11490																									
11500																									
11600																									
11610																									
11620																									

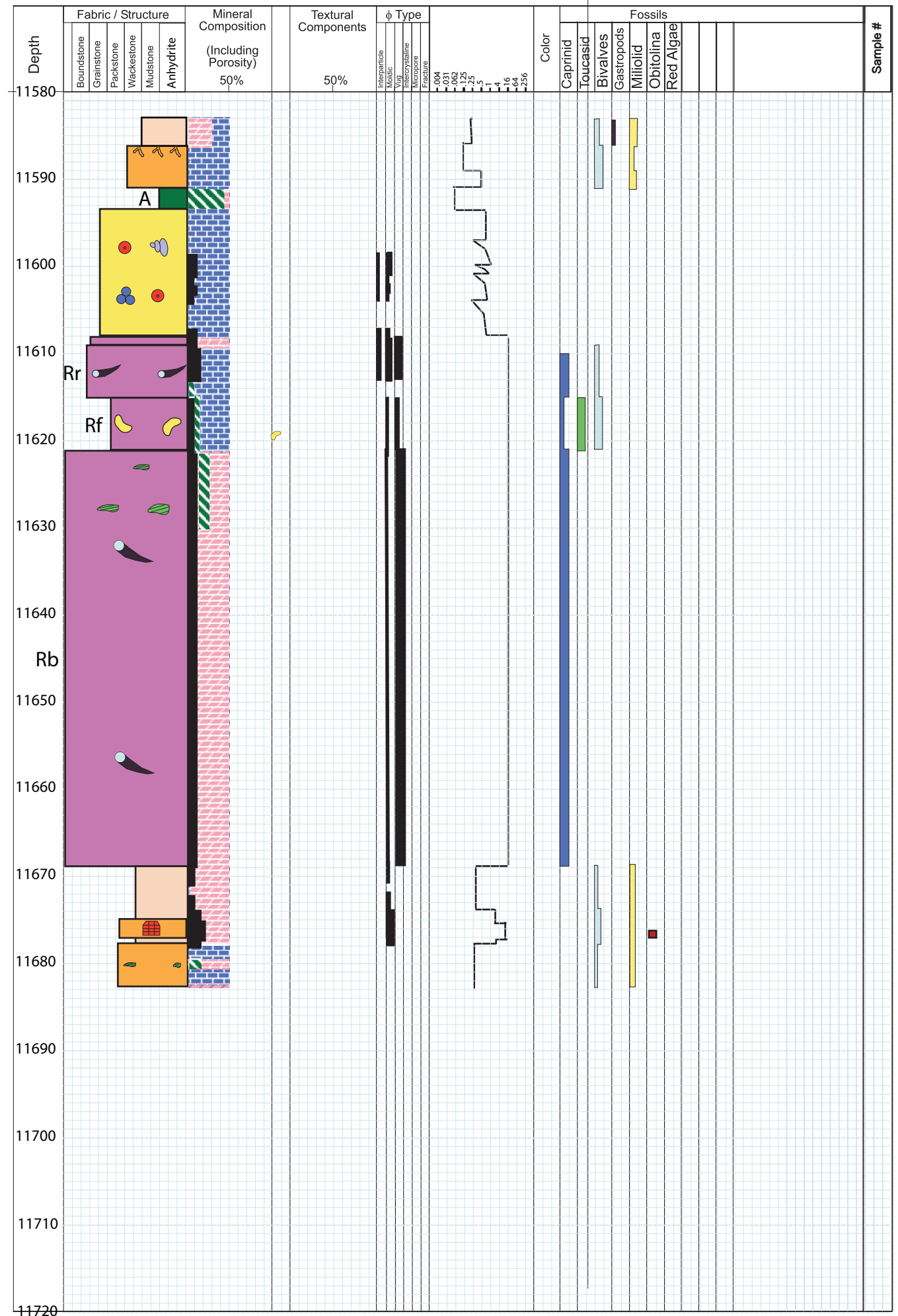
Depth	Fabric / Structure					Mineral Composition (Including Porosity) 50%	Textural Components 50%	φ Type					Color	Fossils										Sample #			
	Boundstone	Grainstone	Packstone	Wackestone	Mudstone			Anhydrite	Interparticle	Moldic	Vug	Crystalline		Micro-pore	Fracture	Caprinid	Toucasid	Bivalves	Gastropods	Miliolid	Obitolina	Red Algae					
11730																											
11740																											
11750																											
11760																											
11770																											
11780																											
11790																											
11800																											
11810																											
11820	W1																										
11830	M1																										
		ES →																									
		ES →																									
		ES →																									
		ES →																									
11840	W1																										
11850	M1																										
	R2																										
	R1																										
11860																											
11870																											

69

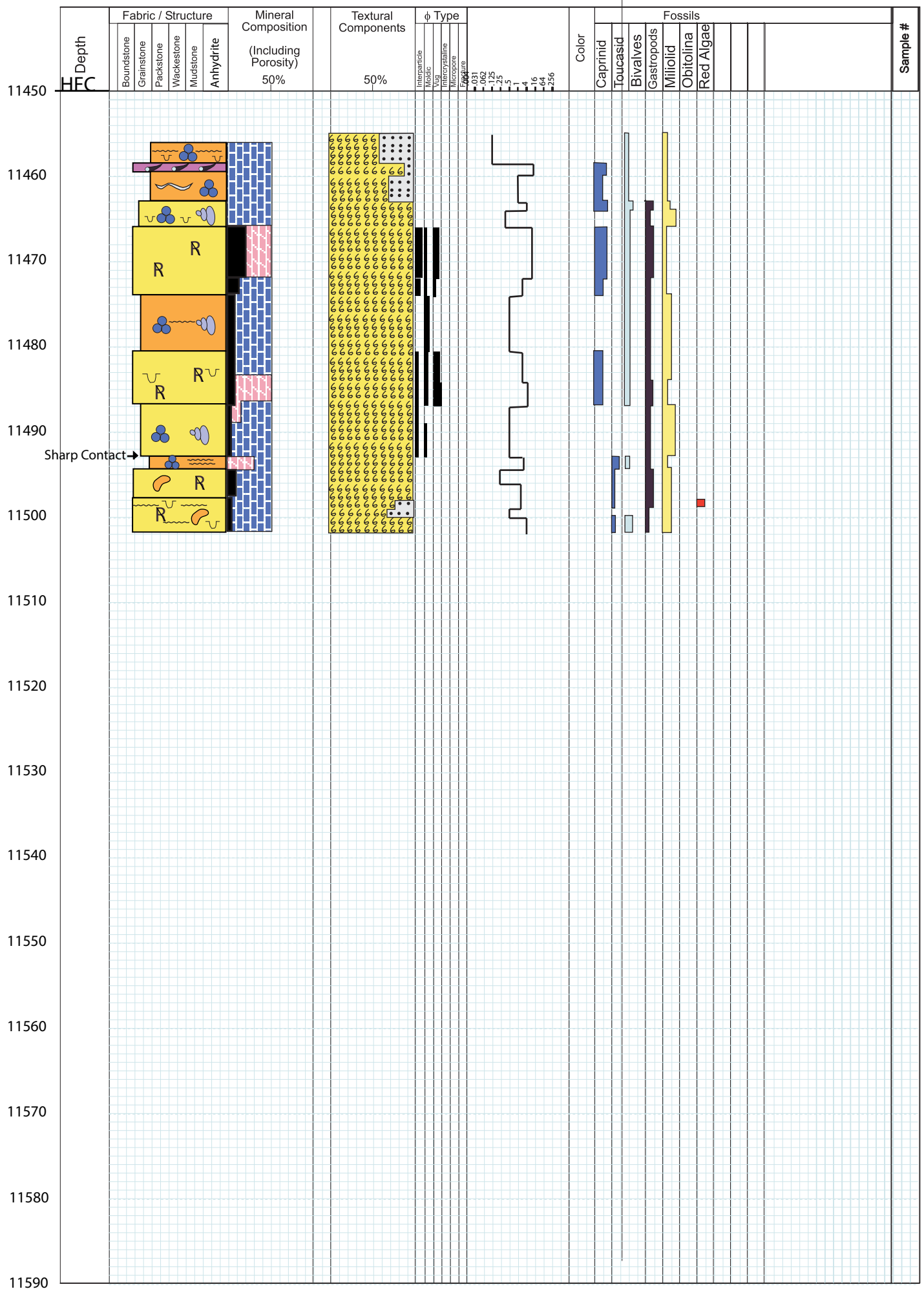
Location: Collier, FL

Logged By: CXL

Date:



Depth HFC	Fabric / Structure					Mineral Composition (Including Porosity) 50%	Textural Components 50%	φ Type						Color	Fossils										Sample #					
	Boundstone	Grainstone	Packstone	Wackestone	Mudstone			Anhydrite	Interparticle	Moldic	Vug	Crystaline	Microspore		Fracture	0.031	0.062	0.125	0.25	0.5	1	4	16	64		256				
11550																														
11560																														
11570																														
11580																														
11590																														
11600																														
11610																														
11620																														
11630																														
11640																														
11650																														
11660																														
11670																														
11680																														
11690																														



Depth	Fabric / Structure					Mineral Composition (Including Porosity) 50%	Textural Components 50%	φ Type					Color	Fossils										Sample #												
	Boundstone	Grainstone	Packstone	Wackestone	Mudstone			Anhydrite	Interparticle	Moldic	Vug	Crystaline		Microzone	Fracture	0.04	0.031	0.062	0.125	0.25	0.5	1	4		16	64	256	Caprinid	Toucasid	Bivalves	Gastropods	Miliolid	Obitolina	Red Algae		
11580																																				
11360																																				
11370																																				
11380																																				
11390																																				
11400																																				
11410																																				
11420																																				
11430																																				
11440																																				
11450																																				
11460																																				
11470																																				
11480																																				
11490																																				

References

- Aconcha, E. (2008). *Integrated core, well log, and seismic interpretation of Albian patch reefs in Maverick Basin, SW Texas*. University of Texas at Austin: Thesis.
- Aisner. (2010). *Patch-reef and ramp interior facies architecture of the Early Albian Mural Limestone, Southeastern Arizona*. Master's Thesis, the University of Texas at Austin, 161 P.
- Aisner, R., & Kerans, C. (2010). *The Mural Limestone of Arizona: An Outcrop Analog for the Aptian-Albian Patch-Reef Reservoirs of the Maverick Basin*. Austin, Texas 78713: Bureau of Economic Geology, the University of Texas at Austin.
- Alsharhan, A. (1995). Facies variation, diagenesis, and exploration potential of the Cretaceous rudist-bearing carbonates of the Arabian Gulf. *AAPG Bulletin* v. 79 no. 4, 531-550.
- Applegate, A. V. (1978). *Future Oil Potential of the Lower Cretaceous Sunniland Formation in South Florida*. Tallahassee, Florida: Florida Department of Natural Resources, Bureau of Geology.
- Bebout, D. G., & Loucks, R. G. (1974). *Stuart City Trend Lower Cretaceous, South Texas: A Carbonate shelf-margin model for hydrocarbon exploration, report of investigations No. 78*. The University of Texas at Austin.
- Blakey, R. (2014, November). *Paleogeographic and Geologic Evolution of North America*. Retrieved from Paleogeography: <https://www2.nau.edu/rcb7/namK115.jpg>
- BOEM. (2015, July 1). *Gulf of Mexico Region Leasing Information*. Retrieved from Bureau of Ocean Energy Management: <http://www.boem.gov/Gulf-of-Mexico-Region-Leasing-Information/>
- Bralower, T. (1999). The record of global change in Mid-Cretaceous (Barremian-Albian) sections from the Sierra Madre, northeastern Mexico. *Journal of Foraminiferal Research*, 29, 418-437.
- Coffin, M., & Eldholm, O. (1994). Large Igneous Provinces Crustal Structure, Dimensions, and External Consequences. *Reviews of Geophysics*, 32, 1-36.
- Dupraz, C., & Strasser, A. (2002). Nutritional models in coral-microbiolite reefs (Jurassic, Oxfordian, Switzerland): evolution of trophic structures as a response to environmental change. *Palaaios*, v.17 no.5, 449-471.

- Erba, E. (1994). Nannofossils and superplumes: The Early Aptian "nannoconid crisis". *Paleoceanography*, 9, 483-501.
- Erba, E. (2010). Calcareous nannoplankton response to surface-water acidification around Oceanic Anoxic Event 1a. *Science*, 329, 428-432.
- Erbacher, J., Thurow, J., & Littke, R. (1996). Evolution patterns of radiolaria and organic matter variations: A new approach to identify sea-level changes in Mid-Cretaceous pelagic environments. *Geology*, 24, 499-502.
- Faulkner, B. M. (1986). Hydrocarbon Exploration Evaluation of the Pulley Ridge Area, Offshore South Florida Basin. *Transactions-Gulf Coast Association of Geological Societies Volume XXXVI*, 83-95.
- Feitz, R. P. (1976). Recent Developments in Sunniland Exploration of South Florida. *Transactions-Gulf Coast Association of Geological Societies Volume XXVI*, 74-78.
- Ferber, R. J. (1985). Depositional Environments of the Sunniland Formation and Diagenetic Characteristics of the Productive Facies, Lehigh Park Field, Florida. *Gulf Coast Association of Geological Societies Transactions*, v. 35, 365.
- GIS Solutions of Florida, H. (2015). *Oil Fields in the Sunniland Trend of South Florida*. Retrieved from Collier Resources Company: Energy balanced with environment: http://www.collierresources.com/Portals/CRC/pdf/Oill-Field-Map_05-2010_V2.pdf
- Gregg, A. (2014). *Tectonic Evolution of the West Florida Basin, Eastern Gulf of Mexico*. Tuscaloosa, Alabama: The University of Alabama.
- Griffin, G. M. (1969). Geothermal Gradients in Florida and Southern Georgia . *Transactions-Gulf Coast Association of Geological Societies Volume XIX*, 189-193.
- Hamdan, A., & Alsharhan, A. (1991). Paleoenvironments and paleoecology of the rudists in the Shuaiba Formation (Aptian) United Arab Emirates. *Journal of African Earth Sciences*, v.12, no.4, 569-581.
- Haq, B., Hardenbol, J., & Vail, P. (1988). Mesozoic and Cenozoic Chronostratigraphy and Cycles of Sea-level Change. *SEPM Special Publication No. 42*.

- Hillgartner, H., van Buchem, F., Gaumet, F., Razin, P., Pittet, B., Grottsch, J., & Droste, H. (2003). The Barremian-Aptian evolution of the Eastern Arabian carbonate platform margin (Northern Oman). *Journal of Sedimentary Geology*, v73, no.5, 756-773.
- Immenhauser, A., & Scott, R. (2002). An estimate of Albian sea-level amplitudes and its implication for the duration of stratigraphic hiatuses. *Sedimentary Geology*, V.152, 19-28.
- Johnson, C. (2002). The Rise and Fall of Rudist Reefs. *American Scientist*, 148.
- Jones, C., & Jenkyns, H. (2001). Seawater strontium isotopes, oceanic anoxic events, and seafloor hydrothermal activity in the Jurassic and Cretaceous . *American Journal of Science*, 301, 112-149.
- Kerans. (2014). *Lower Cretaceous (Mid-Albian) Lower Glen Rose Biostrome in Northern Maverick County, Texas*. Austin, TX: Texas Bureau of Economic Geology.
- Kerans, & Zahm. (2007). *Cretaceous Ramp Margin Rudist Buildup, Pipe Creek Area*. Austin, TX: Texas Bureau of Economic Geology.
- Kerans, C., & Loucks, R. (2002). Stratigraphic Setting and Controls on Occurrence of High-Energy Carbonate Beach Deposits: Lower Cretaceous of the Gulf of Mexico. *Gulf Coast Association of Geological Societies Transactions*, Volume 52, 517.
- Larson, R. (1991). Latest Pulse of Earth: Evidence for a mid-Cretaceous superplume. *Geology*, 547-550.
- Leckie, R. (2002). Oceanic anoxic events and plankton evolution: biotic response to tectonic forcing during the Mid-Cretaceous. *Paleoceanography*, 17.
- Lloyd, J., & Applegate, A. (1985). *1985 Florida Petroleum Production and Exploration*. Tallahassee: Florida Geological Survey.
- Loucks. (1977). *Porosity Development and Distribution in Shoal-water Carbonate Complexes - Subsurface Pearsall Formation (Lower Cretaceous) south Texas*. Austin, TX: Texas Bureau of Economic Geology.
- Loucks. (1985). Vertical facies sequences of the Sunniland and Punta Gorda Formations in the Lower Cretaceous south Florida embayment: Natural Resource Management Corporation No. 31-2 Alico core. *Gulf Coast Association of Geological Societies*, 111-118.

- Loucks, & Tinker. (2014). *Lower Cretaceous (Lower Albian) Lower Glen Rose Shelf-Interior Shoal-water Complex in Frio County, Texas*. Austin, TX: Texas Bureau of Economic Geology.
- Loucks, R., & Longman, M. (1982). Lower Cretaceous Ferry Lake anhydrite, Fairway field, East Texas: product of shallow-subtidal deposition. In C.R. Handford, R.G. Loucks and G.R. Davies (Eds.), *depositional and diagenetic spectra of evaporites . Journal of the Middle East Petroleum Geosciences*, 130-173.
- Lucia, F. (1995). Rock-fabric/petrophysical classification of carbonate pore space for reservoir characterization. *AAPG Bulletin*, v.79, 1275-1300.
- Means, J. A. (1976). *Sunoco Felda and West Sunoco Felda Fields Hendry, Collier aand Lee Counties, Florida*. Dallas, Texas: Sun Oil Company.
- Miller, K. (2005). The Phanerozoic record of global sea-level change. *Science* 310, 530-545.
- Mitchell-Tapping, H. (2000). Evidence of Volcanic Activity during the Cretaceous in the Sunniland Formation of Southwestern Florida: A new Oil Exploration Play. *Gulf Coast Association of Geological Societies Transactions, Volume L*, 743-750.
- Mitchell-Tapping, H. J. (1984). Petrology and Depositional Environment of the Sunniland Producing Fields of South Florida. *Transactions-Gulf Coast Association of Geological Societies Volume XXXIV*, 157-173.
- Mitchell-Tapping, H. J. (1985). Petrology of the Sunniland, Forty Mile Bend, and Bear Island Fields of South Florida. *Transactions-Gulf Coast Association of Geological Societies Volume XXXV*, 233-242.
- Mitchell-Tapping, H. J. (1986). Exploration Petrology of the Sunoco Felda Trend of South Florida . *Transactions-Gulf Coast Association of Geological Societies Volume XXXVI*, 241-256.
- Mitchell-Tapping, H. J. (1987). Application of the Tidal Mudflat Model to the Sunniland Formation of South Florida . *Transactions-Gulf Coast Association of Geological Societies Volume XXXVII*, 415-426.
- Mitchell-Tapping, H. J. (1996). Historical Interval and Name Changes of the Southern Florida Sunniland Formation . *Transactions-Gulf Coast Association of Geological Societies* , 301-306.

- Mitchell-Tapping, H. J. (2002). Exploration Analysis of Basin Maturity in the South Florida Sub-Basin. *Transactions-Gulf Coast Association of Geological Societies Volume 52*, 753-764.
- Mitchell-Tapping, H. J. (2003). Exploration of the Sunniland Formation of Southern Florida. *Transactions-Gulf Coast Association of Geological Societies Volume 53*, 599-609.
- Mitchell-Tapping, H. J. (2003). Rudistids of the South Florida Lower Cretaceous Sunniland Formation . *Transactions-Gulf Coast Association of Geological Societies*, 584-598.
- Montgomery, S. L. (1987). *Petroleum Frontiers*. Denver, Colorado: Petroleum Information Corporation.
- Oglesby, W. R. (1965). *Folio of South Florida Basin-A preliminary study: Florida Geological Survey Map Series No. 19*, 3P.
- Oglesby, W. R. (1967). A Gravity Profile of the South Florida Shelf. *Transactions-Gulf Coast Association of Geological Societies Volume XVII*, 278-286.
- Page, G., & Miller, S. (2002). Atlas of Log Responses - The Changing Face of Formation Evaluation. Baker Hughes.
- Palacas, J. G. (1978). Preliminary Assessment of Organic Carbon Content and Petroleum Source Rock Potential of Cretaceous and Lower Tertiary Carbonates, South Florida Basin. *Transactions-Gulf Coast Association of Geological Societies Volume XXVIII*, 357-381.
- Palacas, J. G. (1984). *South Florida Basin-A Prime Example of Carbonate Source Rocks of Petroleum*. Denver, Colorado: U.S. Geological Survey, Denver Federal Center.
- Phelps, R. (2011). *Middle-Hauterivian to Lower-Campanian Sequence Stratigraphy and Stable Isotope Geochemistry of the Comanche Platform, South Texas*. The University of Texas at Austin.
- Phelps, R. (2014). Oceanographic and eustatic control of carbonate platform evolution and sequence stratigraphy on the Cretaceous (Valanginian-Campanian) passive margin, northern Gulf of Mexico. *Sedimentology*, 461-496.
- Pollastro, R. M. (1995). *1995 USGS National Oil and Gas Play-Based Assessment of the South Florida Basin, Florida Peninsula Province*. Washington, DC: USGS.

- Pollastro, R., & Viger, R. (1998). *Maps Showing Hydrocarbon Plays of the Florida Peninsula, USGS Petroleum Province 50*. U.S. Geological Survey.
- Pressler, E. D. (1947, October). Geology and Occurrence of Oil in Florida . *Bulletin of the American Association of Petroleum Geologists Volume 31, No. 10*, pp. 1851-1862.
- Puri, H. S., & Banks, J. E. (1959). Structural Features of the Sunniland Oil Field, Collier County, Florida. *Transactions-Gulf Coast Association of Geological Societies Volume IX*, 121-130.
- Rainwater, E. H. (1971). *Possible Future Petroleum Potential of Peninsular Florida and Adjacent Continental Shelves*. Houston, Texas.
- Riccardo, C., & Dario, S. (1995). *Rudists and Facies of the Periadriatic Domain*. San Donato Milanese: AGIP.
- Richard F., I., & Clyde H., M. (1983). Chapter 5 Beach Environment. In *Carbonate Depositional Environments* (p. 255). Tulsa, Oklahoma: The American Association of Petroleum Geologists.
- Richards, J. A. (1988). Depositional History of the Sunniland Limestone (Lower Cretaceous), Raccoon Point Field, Collier County, Florida. *Transactions-Gulf Coast Association of Geological Societies Volume XXXVIII*, 473-483.
- Sahagian, D., Pinous, O., Olferiev, A., & Zakharov, V. (1996). Eustatic Curve for the Middle Jurassic--Cretaceous Based on Russian Platform and Siberian Stratigraphy: Zonal Resolution. *AAPG Bulletin*, 1433-1458.
- Scholle, P., Bebout, D., & Moore, C. (1983). *Carbonate Depositional Environments* : *AAPG Memior #33*, 708 P.
- Scott, R. (1979). Depositional Models of Early Cretaceous Coral-Algal-Rudist Reefs, Arizona. *AAPG Bulletin V.63, Issue. 7*, 1108-1127.
- Scott, R. W. (2002). Albian Caprinid Rudists from Texas Re-evaluted. *Journal of Paleontology*, 408-423.
- Shinn, E. (1983). Tidal Flat Environment. In Scholle, *Carbonate Depositional Environments. AAPG Memoir 33*. (pp. 171-210).
- Tyler, A. N. (1976). *Sunoco-Felda Field, Hendry and Collier Counties, Florida*.

- Winston, G. O. (1971). Regional Structure, Stratigraphy, and Oil Possibilities of the South Florida Basin. *Transactions-Gulf Coast Association of Geological Societies Volume 21*, 15-29.
- Winston, G. O. (1976). Six Proposed Formations in the Undefined Portion of the Lower Cretaceous Section in South Florida . *Transactions-Gulf Coast Association of Geological Societies Volume XXVI*, 69-72.